Atmos. Chem. Phys. Discuss., https://doi.org/10.5194/acp-2018-922
Manuscript under review for journal Atmos. Chem. Phys.
Discussion started: 15 October 2018

Introduction to Special Issue - In-depth study of air pollution sources and processes within Beijing and its surrounding region (APHH-Beijing)

Zongbo Shi[1,2*], Tuan Vu[1], Simone Kotthaus[3,4], Sue Grimmond[3], Roy M. Harrison[1†], Siyao Yue[5], Tong Zhu[6], James Lee[7,8], Yiqun Han[6,9], Matthias Demuzere[10], Rachel E Dunmore[7], Lujie Ren[2,5], Di Liu[1], Yuanlin Wang[5,11], Oliver Wild[11], James Allan[12,13], Janet Barlow[3], David Beddows[1], William J, Bloss[1], David Carruthers[14], David C Carslaw[7,15], Lia Chatzidiakou[16], Leigh Crilley[1], Hugh Coe[12], Tie Dai[5], Ruth Doherty[17], Fengkui Duan[18], Pingqing Fu[2,5], Baozhu Ge[5], Maofa Ge[19], Daobo Guan[20], Jacqueline F. Hamilton[7], Kebin He[18], Matthew Heal[17], Dwayne Heard[21], C Nicholas Hewitt[11], Min Hu[6], Dongsheng Ji[5], Xujiang Jiang[18], Rod Jones[16], Markus Kalberer[16,a], Frank J Kelly[9], Louisa Kramer[1], Ben Langford[22], Chun Lin[17], Alastair C Lewis[7], Jie Li[5], Weijun Li[23], Huan Liu[18], Miranda Loh[24], Keding Lu[6], Graham Mann[25], Gordon McFiggans[12], Mark Miller[26], Graham Mills[27], Paul Monk[28], Eiko Nemitz[22], Fionna O'Connor[29], Bin Ouyang[11,16], Paul I. Palmer[17], Carl Percival[12,b], Olalekan Popoola[16], Claire Reeves[27], Andrew R Rickard[7,8], Longyi Shao [30], Guangyu Shi[5], Dominick Spracklen[25], David Stevenson[17], Yele Sun[5], Zhiwei Sun[31], Shu Tao[32], Shengrui Tong[19], Qingqing Wang[5], Wenhua Wang[30], Xinming Wang[33], Zifang Wang[5] Lisa Whalley[21], Xuefang Wu[1], Zhijun Wu[6], Pinhua Xie[34], Fumo Yang[35], Qiang Zhang[36], Yanli Zhang[33], Yuanhang Zhang[6], Mei Zheng[6]

[1] School of Geography Earth and Environmental Sciences, University of Birmingham, UK
[2] Institute of Surface Earth System Science, Tianjin University, China
[3] Department of Meteorology, University of Reading, UK
[4] Institut Pierre Simon Laplace, Ecole Polytechnique, France
[5] Institute of Atmospheric Physics, Chinese Academy of Sciences, Beijing, China
[6] College of Environmental Sciences and Engineering, Peking University, Beijing, China
[7] Wolfson Atmospheric Chemistry Laboratories, Department of Chemistry, University of York, York, UK
[8] National Centre for Atmospheric Science, University of York, York, UK
[9] Analytical & Environmental Sciences Division, King's College London, London, UK
[10] Laboratory of Hydrology and Water Management, Ghent University, Coupure Links 653, B-9000 Ghent, Belgium
[11] Lancaster Environment Centre, Lancaster University, Lancaster, UK
[12] School of Earth and Environmental Sciences, The University of Manchester, Manchester, UK
[13] National Centre for Atmospheric Science, The University of Manchester, Manchester, UK
[14] Cambridge Environmental Research Consultants, Cambridge UK
[15] Ricardo Energy & Environment, Harwell, Oxfordshire
[16] Department of Chemistry, University of Cambridge, Cambridge, UK
[17] School of Geosciences, University of Edinburgh, Edinburgh, UK
[18] School of Environment, Tsinghua University, Beijing China
[19] Institute of Chemistry, Chinese Academy of Sciences, Beijing, China
[20] School of International Development, University of East Anglia, Norwich, UK
[21] Department of Chemistry, University of Leeds, Leeds, UK
[22] Centre for Ecology & Hydrology, Penicuik, UK

[*] Corresponding Author: Zongbo Shi (email: z.shi@bham.ac.uk)
[†] Also at: Department of Environmental Sciences / Center of Excellence in Environmental Studies, King Abdulaziz University, PO Box 80203, Jeddah, 21589, Saudi Arabia
[a] Now at: University of Basel, Department of Environmental Sciences, Klingelbergstrasse 27, 4056 Basel, Switzerland
[b] Now at Jet Propulsion Laboratory, 4800 Oak Grove Drive, Pasadena, CA 91109, USA

Atmos. Chem. Phys. Discuss., https://doi.org/10.5194/acp-2018-922
Manuscript under review for journal Atmos. Chem. Phys.
Discussion started: 15 October 2018

[23] School of Earth Sciences, Zhejiang University, Hangzhou, China
[24] Institute of Occupational Medicine (IOM), Edinburgh, UK
[25] School of Earth and Environment, University of Leeds, Leeds, UK
[26] Centre for Cardiovascular Science, Queen's Medical Research Institute, University of Edinburgh, Edinburgh, UK
[27] School of Environmental Studies, University of East Anglia, Norwich, UK.
[28] Department of Chemistry, University of Leicester, Leicester, UK
[29] Hadley Centre, Met Office, Reading, UK
[30] State Key Laboratory of Coal Resources and Safe Mining & College of Geosciences and Surveying Engineering, China University of Mining and Technology (Beijing)
[31] School of Public Health, Capital Medical University, Beijing, China
[32] College of Urban and Environmental Sciences, Peking University, Beijing, China
[33] Guangzhou Institute of Geochemistry, Chinese Academy of Sciences, Guangzhou, China
[34] Anhui Institute of Optics and Fine optics, Chinese Academy of Sciences, Hefei, China
[35] Department of Environmental Science and Engineering, College of Architecture and Environment, Sichun University, Chengdu, China
[36] Department of Earth System Science, Tsinghua University, Beijing, China

ABSTRACT

APHH-Beijing (Atmospheric Pollution and Human Health in a Chinese Megacity) is an international collaborative project to examine the emissions, processes and health effects of air pollution in Beijing. The four research themes of APHH-China are: (1) sources and emissions of urban atmospheric pollution; (2) processes affecting urban atmospheric pollution; (3) exposure science and impacts on health; and (4) interventions and solutions to reduce health impacts. Themes 1 and 2 are closely integrated and support Theme 3, while Themes 1-3 provide scientific data for Theme 4 on the development of cost-effective solutions. A key activity within APHH-Beijing was the two month-long intensive field campaigns at two sites: (i) central Beijing, and (ii) rural Pinggu. The coordinated campaigns provided observations of the atmospheric chemistry and physics in and around Beijing during November – December 2016 and May- June 2017. The campaigns were complemented by numerical air quality modelling and air quality and meteorology data at the 12 national monitoring stations in Beijing. This introduction paper provides an overview of (i) APHH-Beijing programme, (ii) the measurement and modelling activities performed as part of it in Beijing, and (iii) the air quality and meteorological conditions during the two field campaigns. The winter campaign was characterized by high $PM_{2.5}$ pollution events whereas the summer experienced high ozone pollution events. Air quality was poor during the winter campaign, but less severe than in the same period in 2015 when there were a number of major pollution episodes. $PM_{2.5}$ levels were relatively low during the summer period, matching the cleanest periods over the previous five years. Synoptic scale meteorological analysis suggests that the greater stagnation and weak southerly circulation in November/December 2016 may have contributed to the poor air quality.

1. INTRODUCTION

Air pollution is one of the largest environmental risks. It is estimated that air pollution has led to 7 million premature deaths per year globally (WHO, 2016a, b) and over a million in China (GBD MAPS Working Group, 2016). Air pollution also has significant impact on the healthcare system and ecosystems, which cost about 0.3% of global GDP (OECD, 2016). Air pollution related sickness also reduced productivity and severe hazes lead to closure of transport systems, causing additional damage to the economy. Total economic losses related to China's $PM_{2.5}$ (particulate matter with aerodynamic diameter equal to or less than 2.5 μm) pollution in 2007 amounted to 346 billion Yuan (£39 billions, approximately 1.1% of the national GDP) based on the number of affected Chinese employees whose work time in years was reduced because of mortality, hospital admissions and outpatient visits (Xia et al., 2016).

Although air pollution in developed megacities sometimes breaks country specific limits and WHO guidelines, traditional London or Los Angeles type smogs which occurred in the early and mid-20th centuries are rare in developing cities to the same extent. In the developing countries however, the rush to industrialisation and rapid growth in vehicle populations have led to serious air pollution problems that are more complex than the London or Los Angeles smogs. Air pollution is particularly severe in developing megacities, such as Beijing, where rapid urbanisation has led to a fast increase in pollution emissions (Guan et al., 2014), on top of regional pollution from industrial and other anthropogenic activities.

Considerable research effort has led to huge progress in understanding the sources and pollution processes in megacities in western countries, e.g., major interdisciplinary and multi-institutional programmes in Mexico City, Paris and London in the last few years (Molina et al., 2010; Beekmann et al., 2015; Bohnenstengel et al., 2014). Air pollution in megacities in developing countries, in particular in China have been extensively studied, e.g., in CAREBEIJING (e.g., Liu et al., 2012).

However, our understanding of sources and emissions of key air pollutants such as $PM_{2.5}$ and ozone plus the interaction of physical and chemical processes in the formation of pollution events in developing megacities is still far from being accurate or complete.

Beijing's air pollution is different to that in other heavily studied megacities, such as Paris, Mexico City and London, in a number of ways including the lack of diesel emissions in the inner city, the use of coal in surrounding rural areas for heating and domestic cooking (Tao et al., 2018), the high emissions of air pollutants in neighbouring provinces (Hebei and Tianjin) and the high oxidising power due to the complex chemistry (Zhang et al., 2009; Li et al., 2017; Lu et al., 2018). This makes Beijing a particularly interesting place to study as it provides a new environment to test our understanding of urban pollution processes.

Adverse health effect of air pollution is one of the key motivations to control air pollution. Research has shown that air pollution is one of the leading causes of disease burden in China (GBD MAPS Working Group, 2016). Especially, particulate pollution, the leading cause of severe air pollution events in China, has a significant impact on human health and is associated with high mortality (Zhang et al., 2017a), with considerable proportion of this related to cardiorespiratory diseases (namely stroke, ischemic heart disease, and chronic obstructive pulmonary disease) (Yang et al., 2013; Lozano et al., 2013). Despite this increasing evidence base, the adverse health impact of air pollution remains a complex issue. For instance, the risk assessment of disease burden due to air pollution in China relied largely on the studies undertaken in Europe and North America, which likely over-simplifies estimates due to the difference of race, life style, air pollution settings (Lim et al., 2012). The marked change in air pollution sources and composition between heating and non-heating seasons, and the differences between urban and rural areas may all lead to different biological responses in local residents. However, to date, such comparative investigations are largely lacking.

Atmos. Chem. Phys. Discuss., https://doi.org/10.5194/acp-2018-922
Manuscript under review for journal Atmos. Chem. Phys.
Discussion started: 15 October 2018

A further limitation of such work is the lack of accurate personal exposure estimates which are crucial in high quality health studies. This may be especially true when considering household air pollution (both indoors and outdoors) from traditional biomass and coal stoves which may not be easily captured by ambient located monitoring instruments (Linn et al., 2001; Brook et al., 2002). To address current uncertainties and challenges it is essential to improve understanding of the health impact of air pollution worldwide, and to develop mitigation measures with limited resources on health services.

To address these issues, the UK Natural Environment Research Council (NERC), in partnership with the National Science Foundation of China (NSFC), UK Medical Research Council (MRC) and UK-China Innovation Newton Fund funded a major joint research programme – Atmospheric Pollution and Human Health in a Chinese Megacity (APHH-Beijing). The APHH programme is taking a multi-disciplinary approach to investigating (1) sources and emissions of urban atmospheric pollution; (2) processes affecting urban atmospheric pollution; and (3) the exposure and impacts of air pollution on human health. The scientific understanding from these three themes underpin the development of interventions and solutions to improve air quality and reduce health impacts.

This special issue "In-depth study of air pollution sources and processes within Beijing and its surrounding region (APHH-Beijing)" documents the research outcomes of this APHH-Beijing programme, in particular the atmospheric measurement and modelling aspects. This paper describes the aims and objectives of APHH-Beijing and presents some of the background air quality and meteorology observations that form the basis of data interpretation for the whole programme.

2. APHH-BEIJING PROGRAMME OBJECTIVES

The overall aim of APHH-Beijing is to better understand the sources, atmospheric transformations and health impacts of air pollutants in the Beijing megacity and to improve the capability of forecasting air quality and developing cost-effective mitigation measures. Specific objectives include:

- to determine the emission fluxes of key air pollutants and to measure the contributions of different sources, economic sectors and regional transport to air pollution in Beijing
- to improve understanding of the processes by which pollutants are transformed or removed through transport, chemical reactions and photolysis and the rates of formation and conversion of particulate matter via atmospheric reactions
- to improve understanding on how the detailed properties of particulate matter evolve and can influence their physical properties and behaviour in the atmosphere and elucidate the mechanisms whereby those properties may interact and feedback on urban scale and regional meteorology
- to exploit new satellite observations and regional models to place the *in-situ* campaigns into a wider context
- to determine the exposure of Beijing inhabitants to key health related pollutants using personal air pollution monitors and assess the association between air pollution exposure and key cardiopulmonary measures
- to determine the contribution of specific activities, environments and pollution sources to the personal exposure of the Beijing population to air pollutants derived from outdoor sources
- to enhance our understanding of the health effects in susceptible individuals over time periods when there are large fluctuations in pollutants compared with normal controls, and to identify health outcomes of air pollution.
- to estimate economic loss due to both physical and mental impacts of air pollution and examine how Beijing can improve its air quality more cost effectively

3. RESEARCH THEMES AND INTEGRATION WITHIN THE APHH-BEIJING PROGRAMME

The APHH-Beijing programme has four themes to address specific objectives (Section 2).

3.1 Research Themes

3.1.1 Sources and emissions

This topic is addressed by the AIRPOLL-Beijing (Source and Emissions of Air Pollutants in Beijing) project. AIRPOLL aimed to quantify the emission fluxes of key air pollutants in Beijing and the contributions of different sources, economic sectors and regional transport to air pollution in Beijing. Several science topics addressed individual issues, which are integrated to achieve the overall aims. The project carried out two major field measurement campaigns jointly with the AIRPRO (The integrated Study of **AIR** Pollution **PRO**cesses in Beijing) and AIRLESS (Effects of **AIR** pollution on cardiopu**L**monary dis**E**a**S**e in urban and peri-urban re**S**idents in Beijing) projects (section 3.1.2 and 3.1.3) using sites within Beijing (at the Institute of Atmospheric Physics (IAP)) and in the local region (the rural Pinggu site – see 4.1 for site information). During winter and summer sampling campaigns, AIRPOLL measured the concentrations of key tracers and reactive species indicative of sources and chemical pathways at the ground sites. AIRPOLL also analysed the vertical concentration profiles measured in conjunction with data from monitoring sites across Beijing.

As Beijing is subject to long-range transport of pollutants from neighbouring regions, a key aim was to differentiate advected pollutants from local emissions. Local sources include road traffic, cooking, burning of fossil fuels by industry and for domestic heating. Secondary pollutants are expected to be largely advected, but the geographic scale of Beijing is sufficient for some formation of secondary pollutants within the city.

During the intensive campaigns, the project measured the fluxes of particulate and gaseous air pollutants from ground-level sources by sampling on a tower at the IAP site, which are being compared with estimates taken from the inventory for Beijing. This was complemented by top-down fluxes inferred from satellite data for nitrogen dioxide, sulphur dioxide and formaldehyde, the latter indicative of VOC oxidation processes (Palmer et al., 2003; Fu et al., 2007). Through these means, the emissions inventory are being tested, allowing revisions which are being incorporated into the atmospheric modelling work.

AIRPOLL also made very detailed on-line and off-line measurements of airborne particles. This included continuous measurements of size distributions from 1 nm to >10 µm diameter. Large molecules and molecular clusters were also measured by high resolution mass spectrometry, with a view to better understanding atmospheric nucleation processes. The project monitored the chemical composition of particles in real time by Aerosol Mass Spectrometry and analysed the time-integrated particle samples off-line for major and minor constituents, including organic molecular markers. AIRPOLL determined the carbon-14 in water soluble organic carbon, water insoluble organic carbon and elemental carbon in selected time-integrated particle samples with an aim to differentiate fossil and non-fossil particulate carbon. These data are being brought together for use in receptor modelling of particulate matter sources, which are compared with other estimates of source contributions to particulate matter concentrations.

Measured ground-level concentrations and source apportionment are compared with the predictions of a chemistry-transport model and used to provide a clear distinction between advected regional pollution and the impact of local sources. Divergences between measured and modelled pollutant concentrations will be used to provide critical evaluation of emissions inventories, which will be enhanced iteratively with a view to improving knowledge of the sources and emissions of pollutants affecting air quality in Beijing. Data from AIRPOLL-Beijing measurement and modelling work will also contribute to the aims of the AIRPRO project to elucidate the atmospheric physical and chemical processes determining the measured composition.

3.1.2 Atmospheric processes

AIRPRO aims are to study the basic chemical and physical processes controlling gas and aerosol pollution, localised meteorological dynamics, and the links between them within Beijing's atmosphere. Once released to air, atmospheric processing controls how pollutants are subsequently deposited, transformed into secondary pollutants such as O_3 and particulate matter (PM) or transported away from or within the wider Beijing urban area. Previous studies of pollution in Beijing have shown that it is often perturbation of the physicochemical and dynamic atmospheric conditions that modulate the most severe air quality events, rather than changes in emissions, for example during the development of stable inversions or periods of strong photochemistry. Central to the project were the intensive *in situ* measurements at the IAP meteorological tower (325 m) in Beijing during November-December 2016 and May-June 2017. We made comprehensive and detailed local observations of both primary emitted chemicals and particles, radical intermediates and secondary products, for periods of contrasting local and regional emissions, solar insolation and air temperature. These data allow the performance of local and regional models of air pollution to be robustly tested, both for final regulated pollutant outcomes and at a more mechanistic level.

The observations collected with instruments from multiple Chinese and UK research groups included complementary measurements of key precursor trace gases such as NO_x, HONO, SO_2, CO, O_3, VOCs and SVOCs, gas phase radicals such as OH, HO_2, RO_2, and NO_3, and PM including chemical (both on-line and offline analyses), biological, physical and optical properties. Through multiple co-located surface measurements, there was both instrumental redundancy (e.g. for equipment failures) and capacity to evaluate through inter-comparison some hard-to-measure atmospheric gases such as OH, HO_2, N_2O_5, HCHO and other oxygenated VOCs. The project determined the local *in situ* chemical processing of air pollution in the contrasting winter/summertime periods alongside overall atmospheric reactivity, both day and at night, through a combination of modelling and proxy measurements such as measured ozone production efficiency and OH reactivity.

The IAP tower is critical as it allowed vertical profiles of key pollutants up to 320 m to be obtained and, with additional remote sensing of composition and meteorology, provided insight into boundary layer stability and evolution over the diurnal cycle. Quantification of shallow mixed layers proved to be vital for explaining local surface *in situ* chemical processing and also street level concentrations of relevance to exposure. The potentially significant vertical gradients anticipated in some chemicals and PM properties were further quantified using instruments installed on the tall tower and via profiling gondola measurements. The combined datasets, surface and profiles, provide the basis for evaluation of model performance, and notably comparisons for those intermediates that provide indicators of whether secondary pollution production is being correctly simulated.

3.1.3 Health effects

This theme is addressed by AIRLESS and APIC-ESTEE (Air Pollution Impacts on Cardiopulmonary Disease in Beijing: An integrated study of Exposure Science, Toxicogenomics and Environmental Epidemiology) projects.

AIRLESS aimed to advance air quality and health research in China by bringing together two fields of research that have made rapid advancements in recent years: measurements of a wide range of pulmonary and cardiovascular biomarkers in a panel study and personal monitoring of multiple air pollutants with high spatio-temporal resolution by sensor technology. AIRLESS is also benefiting from the use of an extensive range of pollution metrics collected in the Themes 1 and 2 projects.

These data are being compared with our personal air quality assessments and be used to further understanding of the nature of the air pollution exposures of residents and how this relates to their health status. The APIC-ESTEE study is examining different aspects of air pollution exposure and health, including population studies and toxicology. One aspect of APIC-ESTEE is investigating the relationship between ambient air pollution and personal exposures, and the impacts of both ambient and personal exposures on subclinical health outcomes. Another part of the study is investigating the real-world exposure-reduction and health impact potential of face-masks, a commonly used personal level intervention seen in Beijing. APIC-ESTEE also carried out laboratory toxicology studies to investigate the toxic mechanisms of PM, and a cohort of mothers and children were recruited to investigate relationships between pre-natal air pollution exposures and birth and infancy outcomes.

3.1.4 Solutions

This theme is addressed by INHANCE (Integrated assessment of the emission-health-socioeconomics nexus and air pollution mitigation solutions and interventions in Beijing) project. In recognition of the health and socio-economic issues associated with air pollution, China's State Council authorized a 1.75 trillion Yuan investment package: the Air Pollution Prevention Plan in 2013. INHANCE quantitatively evaluated the performance of China's current air pollution policies wherein the effectiveness of current anti-air pollution measures. INHANCE not only considered physical and mental health impact, direct economic impact, but also the cascading indirect economic losses occurred through inter-industrial and inter-regional linkages on the supply side of the economy. INHANCE established and evaluated interactive relationships among exposure, vulnerability, impact on health, implications for industry and economic consequences.

INHANCE compared and qualitatively assessed air quality policies between Beijing and other cities; undertook policy performance assessment modelling; utilised techno-economic inventories for antipollution measures to conduct micro cost-benefit analysis of new policies; measured health and macroeconomic costs and benefits in mitigating air pollution, and; transformed evidence generated into practical emission alleviation pathways. On these bases, INHANCE will deliver recommendations regarding integrated policy design and an assessment for policy cost-effectiveness.

3.2 Integration Between the Themes

The APHH-Beijing programme is highly integrated to ensure the biggest possible scientific and policy impacts. One of the most significant integration activities between the different themes is the coordinated joint field campaigns at an urban and a rural site in Beijing for Theme 1, 2 and 3 to fully exploit the complementary measurements and expertise by different research groups, which is described in the following sections. Theme 1 & 2 are closely related and in many senses inseparable. For example, our knowledge of the sources and emissions is essential to interpret the processes while knowledge on the atmospheric physical and chemical processes will help us to more accurately quantify the source emissions, both via actual flux-based measurements and model evaluation of the emission inventories. To ensure integration Themes 1 and 2 co-located their rural site at Pinggu as that was selected for the Theme 3 panel study.

Modelling airborne concentrations of air pollutants within Themes 1 and 2 are fully integrated, primarily via the UKCA (UK Chemistry and Aerosol), NAQPMS (Nested Air Quality Prediction Model System) and GEOS-Chem models. Both models simulate spatial and temporal variations of key air pollutants and will be evaluated using the new observations of pollutant emission fluxes, updated emission inventories, three-dimensional air quality low cost sensor measurements, comprehensive composition and physics measurements, as well as new process understandings generated from the APHH-Beijing programme. Furthermore, Themes 1 and 2 ADMS (Atmospheric Dispersion Modelling System) modelling results for the campaign periods facilitate estimation of

Atmos. Chem. Phys. Discuss., https://doi.org/10.5194/acp-2018-922
Manuscript under review for journal Atmos. Chem. Phys.
Discussion started: 15 October 2018

population exposure in Theme 3. Outcomes of Themes 1, 2 and 3 provide Theme 4 with a more accurate estimate of pollution costs and help to develop cost-effective air pollution control measures in Beijing.

The third stream of integration activities involves regular APHH-Beijing programme science and stakeholder engagement meetings to stimulate collaboration and knowledge transfer between different themes and stakeholders. Furthermore, sharing of data was made available via a dedicated depository in Centre for Environmental Data Analysis (www.ceda.ac.uk). All data in the depository will be made publically available by the end of 2022.

4. OVERVIEW OF JOINT FIELD CAMPAIGNS

The two intensive campaigns were from 5th November to 10th December 2016 and 15th May to 22nd June 2017. The campaigns were carried out at both urban and rural sites.

4.1 Site Information

The winter campaign has two main sites. The urban site (39.97N, 116.38 E) is located in the Tower Section of Institute of Atmospheric Physics (IAP), Chinese Academy of Sciences; i.e. at the 325 m meteorological tower. The site, between the fourth and third North ring roads of Beijing (Figure 1), is a residential area. Typical of central Beijing, there are various roads nearby. To the south, north and west there are roads about 150 m away. On site there are 2 to 3 floor buildings to the south, east and west of the tower surrounding by small trees and grasses. There is a canal right to the north of the site. Further to the west is a park covered mainly by conifer pine trees (Yuan Dynasty Wall Heritage).

Atmos. Chem. Phys. Discuss., https://doi.org/10.5194/acp-2018-922
Manuscript under review for journal Atmos. Chem. Phys.
Discussion started: 15 October 2018

Atmospheric Chemistry and Physics Discussions
Open Access
EGU

The rural site in Xibaidian village (40.17N, 117.05 E) in north-eastern Beijing, was collocated with the AIRLESS project cohort. Xibaidian village is about 4 km northwest of Pinggu centre, and about 60 km from IAP. There are many similar small villages nearby. The monitoring station and the clinic used an unoccupied house at the north end of the village away from significant local combustion sources. A two-lane road is about 300 m north to the site. With no centralised heating infrastructure available to the local villages' residents mainly use coal and biomass for heating and cooking in individual homes.

In the summer, an additional site was operated in Gucheng (39.2N 115.7E), Dingxing County, Hebei Province. This site, about 120 km to the southwest of central Beijing, is one of the main highly pollutant transport pathways from Hebei province to Beijing via the southwest passage. The site used a meteorological observatory in a farm field. The nearest town is about 10 km to the northeast. The nearest road is 500 m to the north and the nearest village is about 1 km to the west. Several villages are located around the site.

In addition to the two highly instrumented urban and rural (Pinggu) sites, 21 SNAQ (Sensor Network for Air Quality) boxes, which measure CO, NO, NO_2, CO_2, O_X, size resolved particulates (0.38-17.4 µm), temperature, relative humidity, wind speed and direction (Popoola et al., 2018), were deployed during the summer and winter campaigns across the urban and rural areas of Beijing to map air pollutant variations (red tags, Figure 1). Six additional SNAQ boxes were deployed at six different heights (8, 32, 102, 160, 260, and 320 m) on the IAP tower from 9-23 November 2016 and 25 January-31 December 2017.

Figure 1 also shows the location of the 12 national air quality monitoring stations. Hourly data of criteria air pollutants ($PM_{2.5}$, PM_{10}, SO_2, NO_2, CO and O_3) from January 2013 to December 2017 from the stations were also obtained from official sources by Tsinghua University. The closest air quality station to the urban IAP site is about 3 km away at the Olympic Park.

4.2 Instrumentation

4.2.1 Urban site

Table 1 lists all instruments deployed during the campaigns at the IAP site. The nine instrument containers were at ground level on the campus grass. Their locations are shown in Figure 1c. Online instruments and high volume samplers were deployed at different heights on the meteorological tower. Most instruments ran during both campaigns. Vertical profiles measurements included HONO during pollution events using baskets attached to the tower. Additional online measurements and offline particulate matter samplers were deployed at ground-level, roof of a two storied building to the west (WB) and in a third-floor laboratory at the south-end of the campus. In addition, high, medium and low volume samplers were placed on the roof of WB for offline characterization and source apportionment.

4.2.2 Rural sites

At Pinggu, online instruments (Table 3) were run within an air-conditioned room on the ground floor with inlets on top of the building. High-, medium- and low-volume PM samplers were deployed on a newly modified flat-roof of the single storey building.

At Gucheng (summer only), a high volume Digitel sampler and a single particle sampler were set up on a deserted basketball court. An Aethalometer AE33 was located on top of a container at the edge of the basketball court. CO and O_3 were also measured in a nearby container.

5. AIR QUALITY DURING THE FIELD CAMPAIGNS

5.1 Winter

During the winter sampling campaign the daily average concentration of $PM_{2.5}$ at IAP using Partisol gravimetric measurements was 91.2 µg m^{-3} (Table 4) and 94.0 µg m^{-3} from online FDMS (Filter dynamic measurement system) measurements. The maximum hourly $PM_{2.5}$ concentration was 438 µg m^{-3} (Figure 2). $PM_{2.5}$ concentrations significantly exceeded the both the daily air quality limit of China (75 µg m^{-3}) and WHO (25 µg m^{-3}). During the whole winter campaign period, nearly 50% of the hours had $PM_{2.5}$ mass concentration higher than 75 µg m^{-3} (Figure 2). Online PM_{10} concentration observed at the Olympic Park national air quality monitoring station was up to 560 µg m^{-3} during the campaign with an average of 130.6 µg m^{-3}. Average concentrations of NO_2, O_3, SO_2 and CO were 69.7 ± 33.3, 16.4 ± 17.0 and 14.9 ± 11.1 µg m^{-3} and 1.53 ± 1.02 mg m^{-3}, respectively (Table 4). Most of the criteria pollutants showed a similar temporal pattern (Figure 2), except O_3.

The daily average concentration of $PM_{2.5}$ was 99.7 µg m^{-3} at Pinggu (Table 4; based on Partisol gravimetric measurement) but as high as 114.0 µg m^{-3} from the BAM measurement. The maximum hourly $PM_{2.5}$ concentration was 617 µg m^{-3} (Figure 2). Similarly to IAP, nearly 50% of the hours had $PM_{2.5}$ mass concentrations greater than 75 µg m^{-3}. Average concentrations of NO_2, O_3, SO_2 and CO are 46.4 ± 25.5, 22.3 ± 22.2, and 15.4 ± 6.7 µg m^{-3} and 1.47 ± 1.17 mg m^{-3} (Table 4). $PM_{2.5}$ was slightly higher at the rural site but NO, CO and SO_2 were comparable between the two sites. $PM_{2.5}$ and O_3 each had similar temporal patterns at the urban and rural sites (Figure 2), indicating a synoptic scale meteorological impact. The larger difference in the temporal variation of NO, NO_2 and SO_2 may reflect the varying contribution of more local sources. Large differences in temporal patterns of air pollutants were found on 4 December 2016 when $PM_{2.5}$, SO_2 and NO concentrations were much higher at Pinggu than at IAP.

Diurnal cycles of particles, NO_2 and CO showed no distinct peak but an increment during the nighttime, suggesting the possible impact of boundary layer and/or anthropogenic emissions in winter (Figure 3). The peak NO levels at 7 am are likely caused by the morning rush hour road traffic. $PM_{2.5}$ concentration increased sharply from 6 pm at Pinggu (not shown), suggesting important local emissions, likely domestic heating and cooking. SO_2 and O_3 had their highest levels in mid-morning or at noon (Figure 3).

Variations of particles, NO_x and SO_2 show that higher levels of these pollutants when air masses were from the south or southwest (Figure 4), indicating it was impacted by regional transport. All pollutants, except O_3, had higher mass concentrations when wind speeds were low, suggesting a local source. The NO wind rose suggests a strong local source with little contribution from long-range transport. The O_3 concentration was higher during northerlies and when the concentrations of other pollutants such as NO_x and $PM_{2.5}$ were lower (Figure 4).

SNAQ box measurements at six levels (8 to 320 m) during the winter campaign (Figure 5) have similar overall temporal patterns of CO and NO to that measured by standard gas analyser (Figure 2). In most cases, the air pollutant levels are similar at different levels of the tower. There are notable differences in NO, CO and CO_2 on 11, 12 and 16 / 17 November, which suggests that the mixed layer height was low (e.g., <150 m). Interestingly, the O_x (NO_2 + O_3) levels are relatively homogeneous across the different levels. These measurements have implications on the role atmospheric chemistry play in transformation of species in the boundary layer, and the measurements also provide useful information that confirm mixed layer height determinations from independent methods such as the ceilometer.

Atmos. Chem. Phys. Discuss., https://doi.org/10.5194/acp-2018-922
Manuscript under review for journal Atmos. Chem. Phys.
Discussion started: 15 October 2018

According to the meteorological standards (QX/T113-2010), haze is defined as: i) visibility < 10 km at relative humidity (RH) <80%; or ii) if RH is between 80 and 95%, visibility < 10 km and $PM_{2.5}$ > 75 µg m^{-3}. During the winter campaign 640 of the 1633 h were classified as haze using visibility data from Beijing Capital Airport (Figure 6); within the haze hours 75% had $PM_{2.5}$ greater than 75 µg m^{-3} (Area A, Figure 6) and the rest had a visibility less than 10 km but with a RH <80% (Area B, Figure 6).

Characteristics of five major haze events during the winter campaign (Figure 2) include that $PM_{2.5}$, NO_2, SO_2 and CO had similar trends but O_3 levels dropped to very low concentration (<2 ppb). The events are defined in Table 2.

5.2 Summer

Concentrations of air pollutants excluding ozone during the summer campaign were much lower than in winter (Figure 7, Table 4). Average daily concentration of $PM_{2.5}$ and PM_{10} at IAP were 31.4 ± 14.7 and 74.9 ± 29.3 µg m^{-3} (based on gravimetric method), respectively. These levels were slightly higher than at Pinggu (27.8 ± 13.3 and 62.9 ± 29.3 µg m^{-3}). Concentrations of ozone were four to five times higher during the summer campaigns (106.9 ± 71.6 µg m^{-33} at IAP, and 91.8 ± 62.7 µg m^{-33} at Pinggu) than in the winter campaign. Average concentration of NO_2, SO_2 and CO are 41.3 ± 23.5 and 6.3 ± 6.8 µg $m^{-3}$and 0.61 ± 0.32 ,g m^{-3}at IAP (Table 4). The concentration of NO_2 and CO were lower at Pinggu while that of SO_2 was similar. Most of the criteria pollutants showed a similar temporal pattern (Figure 2), except O_3.

Diurnal patterns of NO, NO_2, and CO at IAP showed a distinct peak in the early morning, suggesting the contribution of traffic emissions (Figure 7). O_3 and O_x concentration peaked in mid-afternoon.

The IAP $PM_{2.5}$ wind rose suggests both local and regional sources (from the south and south-east direction) impact the site (Figure 4). Unlike winter, high ozone concentrations occur during southerlies to southwesterlies, suggesting a regional source of this pollutant. NO and NO_x were largely from local sources during the summer campaign.

Characteristics of two minor haze events (IAP) during the summer campaign (Figure 7) are shown in Table 2.

5.3 Air quality in Wider Beijing Megacity During the Field Campaigns

Average concentrations of air pollutants ($PM_{2.5}$, PM_{10}, NO_2, CO, SO_2 and O_3) at IAP and Pinggu during the two field campaigns were similar to long term averages for these times of year at the 12 national air quality monitoring sites for 2013-2017 (Table 4).

To assess if the IAP air quality is broadly representative of the wider Beijing megacity, variables are correlated with the 12 national air quality station data (Figure 8). A high correlation occurs with $PM_{2.5}$ across all sites except the rural background air quality station at Ming Tombs; PM_{10}, CO and NO_2 at the urban sites are highly correlated but not with the rural and suburban sites suggesting a more local source for these pollutants, comparing to $PM_{2.5}$ and O_3; SO_2 between sites have lower correlation comparing to all other pollutants. The particularly high correlation of $PM_{2.5}$ and O_3 across almost all sites indicates a regional pollution phenomenon for the two pollutants. These results suggested that the air quality at the IAP urban site was broadly consistent with those at the other urban sites.

In general, $PM_{2.5}$ mass concentrations are similar at all the urban sites including IAP but higher than at the suburban and rural background national monitoring site (Ming Tombs, G2) (Figure 9). The Pinggu rural site in this study, has high $PM_{2.5}$ pollution in the winter campaign but has the lowest concentrations during the summer campaign. This suggests that local anthropogenic sources have a major impact on $PM_{2.5}$ at this site during the winter campaigns. Source apportionment results, notably high time resolution data are being used to explore this.

The closest national air quality station (Olympic Park, or Aotizhongxin in Chinese Pingyin) to IAP has highly correlated $PM_{2.5}$ concentration. This suggests that national air quality stations are of sufficient quality to provide valuable information on the spatial and temporal variation of key pollutants to supplement campaign measurements.

Table 4 show the IAP concentrations data for all air quality variables are very close to the 12 national air quality monitoring stations mean. This lends further confidence that the chosen urban site represented well the overall pollution in the Beijing megacity.

6. SYNOPTIC SCALE METEOROLOGY DURING THE FIELD CAMPAIGNS

Given the importance of horizontal advection and wet deposition to air quality in Beijing, the synoptic circulation patterns are clearly important (Miao et al., 2017; Wu et al., 2017; Zhang et al., 2012). To provide the synoptic context of the APHH-China observations, the daily mesoscale flow patterns are classified (Section 6.1) and put into context using a 30-year climatology (Section 6.2).

6.1 Synoptic Circulation Types

Circulation types (CT) are classified using the classification software by the COST Action 733 “Harmonisation and Applications of Weather Type Classifications for European regions” (Philipp et al., 2010) with (ECMWF Re-Analysis) ERA-Interim 6-h 925 hPa geopotential reanalysis data (Dee et al., 2011) at its native 0.75° spatial resolution for the domain of interest (103-129° E, 31 - 49° N) centred on Beijing (40° N, 116.5° E) covering the period 1988-2017. ERA-Interim 10 m U and V wind components are used to facilitate interpretation of the flow patterns. Of the COST733 methods (Huth et al., 2008; Philipp et al., 2010, 2016; Tveito and Huth, 2016) two are used: T-Mode PCA (Principal Component Analysis) and SANDRA (Simulated Annealing And Diversified RAndomization clustering). The former have been used in Beijing previously (e.g. Miao et al., 2017; Zhang et al., 2012). The latter is considered to perform well in clustering pressure fields and discriminating environmental variables (e.g. Demuzere et al., 2011; Philipp et al., 2016). Classification is performed with the number of CTs ranging from 7 to 18. 11 CTs from the SANDRA method are selected (Figure 11; Table 5) to adequately represent the general flow conditions around Beijing during the 30 y climatology period (Beck and Philipp, 2010). The CTs are re-ordered according to the daily median $PM_{2.5}$ concentration observed at the Olympic Park (i.e. Aotizhongxin) (Figures 1 and 12) in 2013-2017 with the predominant CTs estimated from midday-midday, i.e. with a 12 h time lag.

As expected, the CTs that occurred during the two field campaign periods are different (Figures 12 and 13). During the winter field campaign, most frequent circulation type was CT 10 (25 % of the 6 h periods) and often preceded by a period of CT 11 (total 16%). Circulation types 9-11 are associated with air masses that may stagnate over the Beijing urban area (Figure 11). However, CT 9 did not occur in winter (or the summer) field campaign. CT 1 accounted for 16% of the time, with CT 2 (1 %) are associated with the Asian winter monsoon which brings cold and dry air masses to eastern China. North-westerly flow over Beijing is driven by high pressure in the west of the domain (Figure 11). After these CT 3, 4, 6, and 5 were the most frequent in the winter campaign (12.5, 11.8, 8.3 and 7.6 % of the time, respectively). CTs 3 and 5 are associated with relatively low pressure in the northeast (Sep-May period). CTs 4 and 6 have a further reduction in atmospheric pressure in the NE. The remaining 6 h period was classified as CT 7, which occurs when winds are oriented westward from the Bohai Sea.

During the summer campaign (Figure 12b), the most frequent CT were 5, 8, 6, 7 (34, 32, 12, 11 % of the time, respectively). CT 8, which did not occur during the winter campaign period, is like CT 6 associated with the summer monsoon advecting moist warm air from the South and Southeast (Figure 11). The other two were CT 1 and 4 (7 and 4 %, respectively). During spring and summer (Mar-Aug,) CT 4 winds start to turn over the Yellow Sea, weakening the NW flow over Beijing.

In comparison to the field campaigns, during the period 1988-2017 the CT frequencies range from 7.2% (CT 2, 10) to 12.9% (CT 8) with clear seasonal variations in their occurrence (Figure 13).

6.2 Synoptic circulation and Air Quality

The 11 CTs (Section 6.1) are clearly associated with distinct air quality conditions based on analysis of hourly air quality data for 2013-2017 at one of the national urban air quality station (G4, Olympic Park, Figures 1 and 12). Relatively lower $PM_{2.5}$ concentrations occur (Figure 13b) under NE flow conditions (CTs 1-5), and higher concentrations during southerly flow (CTs 6-8, 10). The highest $PM_{2.5}$ concentrations occur during the heating season associate with stagnation (CT 9, 11). Ozone levels are highest during CTs 5-8 (Figure 13c) as these predominate during spring and summer (Figure 13d).

Similarly, the average mixed layer height observed at IAP (Table 1) varies with season and CT type (Figure 13a). In the Oct 2016 – Sept 2017 period (Figure 13e), the relative frequency of CTs differs slightly from the long-term climatology (Figure 13d). In December 2016, clear air advection from the NE (CTs 1-3) was less frequent than in the 30-y climatology. However, stagnation with a weak southerly component (CTs 9 and 11) was more frequent (Figure 13f), thus favouring haze with a large positive (40%) $PM_{2.5}$ anomaly (Figure 14g, cf. 5 y average, 2013-2017). In June 2017, south-north contrasts in geopotential were apparently reduced so CT 6 was 24% less frequent, while CTs 4, 7, and 8 were more frequent. This had minimal effect of $PM_{2.5}$; the slight increase in O_3 (by 9.5%, Figure 13g) might be explained by associated cloud cover differences.

6.3 Meteorological Conditions During the Field Campaigns

To assess how local-scale flow related to ERA-Interim fields (section 6.1), the link between the coarse gridded data and tower-based sonic anemometer observations is explored based on wind roses (Figure 14). The 30 y climatology (Figure 13a, d) confirms the clear seasonality in wind direction affecting the occurrence of CTs discussed (Sect. 0), i.e. during winter intensive campaign period (5 November – 10 December) north-easterly flow clearly dominates while southerly wind directions are most common during the summer campaign period (15 May – 22 June). The wind roses for winter 2016 and summer 2017 (Figure 14b, e) are slightly nosier, however, indicating similar tendencies as the climatology. The general large-scale patterns are consistent with the in-situ wind measurements (Figure 14c, f). However, a slight diversion towards northerly and south-westerly flow and lower wind speeds occurred in winter and summer (Figures 14c and f), respectively, when compared to the larger scale data (Figures 14b and d). In addition, south-westerly flows were more frequent in winter 2016 (Figures 14b and c) than the 30 year average climatology (Figure 14a), which had the potential to bring more polluted air in the upwind Hebei province to the observation sites in Beijing.

At 102 m, the flow is consistent with northerlies and north-westerlies in the winter campaign and dominantly southerly and easterlies during the summer campaign (Figure 15). The measured hourly mean wind speed, temperature and relative humidity were 3.1 m s^{-1}, 8.3 ^{o}C and 43.8 % in winter, and 3.6 m s, 25 ^{o}C and 46.7 % in summer, respectively. Typical diurnal patterns were observed with higher wind speed and temperature during the day and RH at night. During the winter haze events the 120 m wind speed were low (an average of 1.8 m s^{-1}) and mainly from the south-west direction (Figures 15 and 2).

6.4 Pollution Climatology of the Campaign Periods

To determine how representative the campaign periods were of the selected seasons in Beijing, pollutant levels were compared with those from the same period each year over the 2013-2017 period. The NAQPMS model was run for the full 5-year period driven by NCEP meteorology and using temporally varying emissions for a single year that is broadly representative of 2017 conditions. Use of annually invariant emissions permits the effect of differing meteorology on pollutant levels to be assessed. The frequency distribution of $PM_{2.5}$ for each campaign period for each year is shown in Figure 16. $PM_{2.5}$ in winter 2016 is very similar in characteristics to that in 2014, and both years show 50% greater PM levels than in 2013 or 2017. However, pollutant levels are substantially lower than in the same period in 2015, when three extended pollution episodes led to period-mean $PM_{2.5}$ that was almost twice as large. In contrast, the summer period in 2017 was relatively clean, with $PM_{2.5}$ levels very similar to 2015, and about 25% less than in 2013, 2014 or 2016.

Data depository:

http://catalogue.ceda.ac.uk/uuid/7ed9d8a288814b8b85433b0d3fec0300

ACKNOWLEDGEMENT

Funding is provided by UK Natural Environment Research Council, Medical Research Council and Natural Science Foundation of China under the framework of Newton Innovation Fund (NE/N007190/1 (R Harrison, Z Shi, W Bloss); NE/N007077/1 (W Bloss)); NE/N00700X/1 (S Grimmond), NE/N007018/1 (F Kelly); NSFC Grant 81571130100(T Zhu), NE/N007115/1 (A C Lewis, A R Rickard, D C Carslaw); NE/N006917/1 (J D Lee, J F Hamilton, R E Dunmore); NE/N007123/1 (J Allan, C Percival, G McFiggans, H Coe); NE/N00695X/1 (C Percival, H Coe, G McFiggans, J Allan); NE/N006976/1 (N Hewitt, O Wild); NE/N006925/1 (O Wild); NE/N006895/1 (D Heard, L Whalley); NE/N00714X/1 (D Guan), NE/N007182/1 (M Loh); and NE/N006879/1 (P Palmer). Other Grant supports from Newton Fund/Met Office CSSP-China (S Grimmond; R Doherty and Z Shi), Royal Society Challenge Grant (CHG/R1/17003, Palmer) and NERC (NE/R005281/1, Shi) are acknowledged. Field help from Kjell zum Berge, Ting Sun at Reading University are also acknowledged. Other staff and students at all involving institutions are acknowledged for their contribution to the field campaigns and programme.

AUTHOR CONTRIBUTIONS

ZS drafted the manuscript and is the science coordinator of the APHH-Beijing programme. RMH, KBH, ACL, PQF, TZ, FJK, ML, ZWS, DBG and ST are lead PIs of the five research projects who led the funding applications and the research. They also drafted section 2. TV plotted many of graphs and carried out the data analysis. SK, SG and MD carried out analysis and wrote section 6.1-6.2; and YLW and OW carried out modelling and plotted Figure 16. PFQ, JL and ZT led the air quality measurements at the two measurements sites. SY, JL, RED, LR, DL, JA, DB, WJ, LC, LC, HC, TD, FKD, BZG, JFH, MH, DH, CNH, MH, DSJ, XJJ, RJ, MK, LK, BL, LC, JL, WJL, KDL, GM, MM, GM (Mills), EN, BO, CP, PIP, OP, CR, LYS, YS, SRT, QQW, WHQ, XMW, ZFW, LW, XFW, ZJW, PHX, FMY, QZ, YLZ and MZ contribute to the field observations, laboratory measurements and / or modelling. ZS, SG, RMH., ZT, JL, OW, JA, JB, WJB, DC, DCC, HC, TD, RD, FKD, PQF, MFG, DBG, JFH, KBH, MH, DH, CNH, MH, XJJ, RJ, MK, FJK, LK, ACL, JL, ML, KL, GM (Mann), GM (McFiggans), MM, PM, EN, FO, PIP, CP, CR, ARR, LYS, GYS, DS (Spracklen), DS (Stevenson), YS, ZWS, ST, SRT, XMW, ZFW, LW, ZJW, PHX, QZ, YHZ and MZ contributed to the funding applications, programme meetings and relevant programme research and/or supervision.

REFERENCES

Beck, C. and Philipp, A.: Evaluation and comparison of circulation type classifications for the European domain, Phys. Chem. Earth, Parts A/B/C, 35, 374-387, 2010.

Beekmann, M., Prévôt, A. S. H., Drewnick, F., Sciare, J., Pandis, S. N., Denier van der Gon, H. A. C., Crippa, M., Freutel, F., Poulain, L., Ghersi, V., Rodriguez, E., Beirle, S., Zotter, P., von der Weiden-Reinmüller, M. Bressi, S.-L.,, Fountoukis, C., Petetin, H., Szidat, S., Schneider, J., Rosso, A., El Haddad, I., Megaritis, A., Zhang, Q. J., Michoud, V., Slowik, J. G., Moukhtar, S., Kolmonen, P., Stohl, A., Eckhardt, S., Borbon, A., Gros, V., Marchand, N., Jaffrezo, J. L., Schwarzenboeck, A., Colomb, A., Wiedensohler, A., Borrmann, S., Lawrence, M., Baklanov, A. and Baltensperger U.: In situ, satellite measurement and model evidence on the dominant regional contribution to fine particulate matter levels in the Paris megacity. Atmos Chem Phys, 15, 9577-9591, 2015.

Crilley, L.R., Kramer, L., Pope, F.D., Whalley, L.K., Cryer, D.R., Heard, D.E., Lee, J.D., Reed, C., Bloss, W.J.: On the interpretation of in situ HONO observations via photochemical steady state. Fara. Discuss., 189, 191-212,2016.

Bohn, B., Heard, D. E., Mihalopoulos, N., Plass-Dülmer, C., Schmitt, R., and Whalley, L. K.: Characterisation and improvement of $j(O^1D)$ filter radiometers, Atmos. Meas. Tech., 9, 3455-3466, 2016.

Bohnenstengel, S. I., Belcher, S. E., Aiken, A., Allan, J. D., Allen, G., Bacak, A., Bannan, T. J., Barlow, J. F.,Beddows, D. C. S., Bloss, W. J., Booth, A. M., Chemel, C., Coceal, O., Di Marco, C. F., Dubey, M. K., Faloon, K. H., Fleming, Z. L., Furger, M., Gietl, J. K., Graves, R. R., Green, D. C., Grimmond, C. S. B., Halios, C. H.,Hamilton, J. F., Harrison, R. M., Heal, M. R., Heard, D. E., Helfter, C., Herndon, S. C., Holmes, R. E., Hopkins, J. R., Jones, A. M., Kelly, F. J., Kotthaus, S., Langford, B., Lee, J. D., Leigh, R. J., Lewis, A. C., Lidster, R. T.,Lopez-Hilfiker, F. D., McQuaid, J. B., Mohr, C., Monks, P. S., Nemitz, E., Ng, N. L., Percival, C. J., Prevot, A. S. H., Ricketts, H. M. A., Sokhi, R., Stone, D., Thornton, J. A., Tremper, A. H., Valach, A. C., Visser, S., Whalley, L. K., Williams, L. R., Xu, L., Young, D. E. and Zotter, P.: Meteorology, air quality, and health in London: The ClearfLo project, B. Am. Meteorol Soc., 96, 779-804, 2014.

Brook, R. D., Brook, J. R., Urch, B., Vincent, R., Rajagopalan, S. and Silverman F.: Inhalation of fine particulate air pollution and ozone causes acute arterial vasoconstriction in healthy adults. Circulation. 105:1534-1536, 2002.

Coyle, M., Nemitz, E., Storeton-West, R., Fowler, D., and Cape, J. N.: Measurements of ozone deposition to a potato canopy, Agri. Forest Meteoro., 149, 655-666, doi:10.1016/j.agrformet.2008.10.020, 2009.

Chen, Y., Wenger, J. C., Yang, F., Cao, J., Huang, R., Shi, G., Zhang, S., Tian, M., and Wang H.: Source characterization of urban particles from meat smoking activities in Chongqing, China using single particle aerosol mass spectrometry, Environ Pollt, 228, 92-101, 2017.

Cryer, D.R., Measurements of hydroxyl radical reactivity and formaldehyde in the atmosphere, PhD Thesis, University of Leeds, 2016.

Dee, D. P., Uppala, S. M., Simmons, A. J., Berrisford, P., Poli, P., Kobayashi, S., Andrae, U., Balmaseda, M. A., Balsamo, G., Bauer, P., Bechtold, P., Beljaars, A. C. M., van de Berg, L., Bidlot, J., Bormann, N., Delsol, C., Dragani, R., Fuentes, M., Geer, A. J., Haimberger, L., Healy, S. B., Hersbach, H., Hólm, E. V., Isaksen, L., Kållberg, P., Köhler, M., Matricardi, M., McNally, A. P., Monge-Sanz, B. M., Morcrette, J.-J., Park, B.-K., Peubey, C., de Rosnay, P., Tavolato, C., Thépaut, J.-N. and Vitart, F.: The ERA-Interim reanalysis: configuration and performance of the data assimilation system, Q. J. R. Meteorol. Soc., 137, 553-597, 2011.

Demuzere, M., Kassomenos, P. and Philipp, A.: The COST733 circulation type classification software: an example for surface ozone concentrations in Central Europe, Theor. Appl. Climatol., 105, 143-166, 2011.

Deventer, M. J., El-Madany, T., Griessbaum, F., and Klemm, O.: One-year measurement of size-resolved particle fluxes in an urban area, Tellus B: Chemical and Physical Meteorology, 67, 1, 25531, 10.3402/tellusb.v67.25531, 2015.

Du, W., Zhao, J., Wang, Y., Zhang, Y., Wang, Q., Xu, W., Chen, C., Han, T., Zhang, F., Li, Z., Fu, P., Li, J., Wang, Z., and Sun, Y.: Simultaneous measurements of particle number size distributions at ground level and 260 m on a meteorological tower in urban Beijing, China, Atmos. Chem. Phys., 17, 6797-6811, 10.5194/acp-17-6797-2017, 2017.

Duan, J., Qin, M., Ouyang, B., Fang, W., Li, X., Lu, K., Tang, K., Liang, S., Meng, F., Hu, Z., Xie, P., Liu, W., and Häsler, R.: Development of an incoherent broadband cavity-enhanced absorption spectrometer for in situ measurements of HONO and NO_2, Atmos. Meas. Tech., 11, 4531-4543, 2018.

Dunmore, R. E., Hopkins, J. R., Lidster, R. T., Lee, J. D., Evans, M. J., Rickard, A. R., Lewis, A. C., and Hamilton, J. F.: Diesel-related hydrocarbons can dominate gas phase reactive carbon in megacities, Atmos. Chem. Phys., 15, 9983-9996, https://doi.org/10.5194/acp-15-9983-2015, 2015.

Fu, T.M., Jacob, D.J., Palmer, P.I., Chance, K., Wang,Y.X., Barletta, B., Blake, D.R., Stanton,J.C., Pilling, M.J.: Space - based formaldehyde measurements as constraints on volatile organic compound emissions in east and south Asia and implications for ozone. J.Geophys. Res. – Atmos., D06312, doi:10.1029/2006JD007853, 2007.

GBD MAPS Working Group: Burden of Disease Attributable to Coal-Burning and Other Major Sources of Air Pollution in China. Special Report 20, Boston, MA, Health Effects Institute, 2016.

Ge, B., Sun, Y., Liu, Y., Dong, H., Ji, D., Jiang, Q., Li, J., and Wang, Z.: Nitrogen dioxide measurement by cavity attenuated phase shift spectroscopy (CAPS) and implications in ozone production efficiency and nitrate formation in Beijing, China, J. Geophys. Res., 118, 9499–9509, 10.1002/jgrd.50757, 2013.

Gerbig, C., Schmitgen, S., Kley, D., Volz-thomas, and Dewey, K.: An improved fast-response vacuum-UV resonance fluorescence CO instrument, J. Geophys. Res. 104, 1699-1704, 1999.

Guan, D., Su, X., Zhang, Q., Peters, G. P., Liu, Z., Lei, Y. and He K.: The socioeconomic drivers of China's primary $PM_{2.5}$ emission, Environ. Res. Lett, 9, 024010, 2014.

Han, T., Liu, X., Zhang, Y., Qu, Y., Gu, J., Ma, Q., Lu, K., Tian, H., Chen, J., Zeng, L., Hu, M., and Zhu, T.: Characteristics of Aerosol Optical Properties and Their Chemical Apportionments during CAREBeijing 2006, Aerosol Air Qual. Res., 14, 1431–1442, 2014.

Han, T., Xu, W., Li, J., Freedman, A., Zhao, J., Wang, Q., Chen, C., Zhang, Y., Wang, Z., Fu, P., Liu, X., and Sun, Y.: Aerosol optical properties measurements by a CAPS single scattering albedo monitor: Comparisons between summer and winter in Beijing, China, J. Geophys. Res., 122, 2513-2526, 10.1002/2016JD025762, 2017.

Högström, U., and Smedman, A.-S.: Accuracy of Sonic Anemometers: Laminar Wind-Tunnel Calibrations Compared to Atmospheric In Situ Calibrations Against a Reference Instrument, Boundary-Layer Meteoro., 111, 33-54, doi:10.1023/b:boun.0000011000.05248.47, 2004.

Hopkins, J.R., C.E. Jones, and A.C. Lewis, A dual channel gas chromatograph for atmospheric analysis of volatile organic compounds including oxygenated and monoterpene compounds, J. Environ. Monitor., 13, 2268-2276, 2011.

Huang, Z., Zhang, Y., Yan, Q., Zhang Z., and Wang X.: Real-time monitoring of respiratory absorption factors of volatile organic compounds in ambient air by proton transfer reaction time-of-flight mass spectrometry, J. Hazard. Mater., 320, 547-555, 2016.

Huth, R., Beck, C., Philipp, A., Demuzere, M., Ustrnul, Z., Cahynová, M., Kyselý, J. and Tveito, O. E.: Classifications of atmospheric circulation patterns, Ann. N. Y. Acad. Sci., 1146, 105-152, 2008.

Johnson, T., Capel, J., and Ollison, W.: Measurement of microenvironmental ozone concentrations in Durham, North Carolina, using a 2B Technologies 205 Federal Equivalent Method monitor and an interference-free 2B Technologies 211 monitor, J. Air & Waste Manag. Asso., 64, 360-371, doi:10.1080/10962247.2013.839968, 2014.

Junninen, H., Ehn, M., Petaja, T., Luosujarvi,L., Kotiaho, T., Kostiainen, R., Rohner, U., Gonin, M., Fuhrer, K., Kulmala, M., and Worsnop,D. R.: A high-resolution mass spectrometer to measure atmospheric ion composition, Atmos. Measure.Tech., 3, 1039–1053, 2010.

Kotthaus, S. and Grimmond, C. S. B.: Atmospheric boundary layer characteristics from ceilometer measurements part 1: A new method to track mixed layer height and classify clouds, Q. J. R. Meteorol. Soc., doi:10.1002/qj.3299, 2018a.

Kotthaus, S. and Grimmond, C. S. B.: Atmospheric boundary layer characteristics from ceilometer measurements part 2: Application to London's urban boundary layer, Q. J. R. Meteorol. Soc., doi:10.1002/qj.3298, 2018b.

Le Breton, M., Bacak, A., Muller, J. B. A., Bannan, T. J., Kennedy, O., Ouyang, B., Xiao, P., Bauguitte, S. J.-B., Shallcross, D. E., Jones, R. L., Daniels, M. J. S., Ball, S. M., Percival, C. J.: The first airborne comparison of N2O5 measurements over the UK using a CIMS and BBCEAS during the RONOCO campaign, Anal. Methods, 6, 9731-9743, 2014.

Le Breton, M., Wang, Y., Hallquist, Å. M., Pathak, R. K., Zheng, J., Yang, Y., Shang, D., Glasius, M., Bannan, T. J., Liu, Q., Chan, C. K., Percival, C. J., Zhu, W., Lou, S., Topping, D., Wang, Y., Yu, J., Lu, K., Guo, S., Hu, M., and Hallquist, M.: Online gas- and particle-phase measurements of organosulfates, organosulfonates and nitrooxy organosulfates in Beijing utilizing a FIGAERO ToF-CIMS, Atmos. Chem. Phys., 18, 10355-10371, 2018.

Li, M., Liu, H., Geng, G., Hong, C., Liu, F., Song, Y., Tong, D., Zheng, B., Cui H., Man, H., Zhang, Q., and He, K.: Anthropogenic emission inventories in China: a review, Nat. Sci. Rev., 4, 834-866, 2017.

Li, Z., Hu, R., Xie, P., Chen, H., Wu, S., Wang, F., Wang, Y., Ling, L., Liu, J., and Liu W.: Development of a portable cavity ring down spectroscopy instrument for simultaneous, in situ measurement of NO_3 and N_2O_5, Optics Express, 26, A433-A449, 2018.

Liang, P., Zhu, T., Fang, Y., Li, Y., Han, Y., Wu, Y., Hu, M., and Wang, J.: The role of meteorological conditions and pollution control strategies in reducing air pollution in Beijing during APEC 2014 and Victory Parade 2015, Atmos. Chem. Phys., 17, 13921-13940, 2017.

Lin, W., Huang, W., Zhu, T., Hu, M., Brunekreef, B., Zhang ,Y., Liu, X., Cheng, H., Gehring, U., Li, C., and Tang, X.: Acute respiratory inflammation in children and black carbon in ambient air before and during the 2008 Beijing Olympics, Environ. Health Perspect., 119, 1507-12, 2011.

Lim, S.S., Vos, T., Flaxman, A.D., Danaei, G., Shibuya, K., Adair-Rohani, H., et al. 2012. A comparative risk assessment of burden of disease and injury attributable to 67 risk factors and risk factor clusters in 21 regions, 1990-2010: A systematic analysis for the global burden of disease study 2010, Lancet 380, 2224-2260, 2012..

Linn, W. S. and Gong, Jr., H.: Air pollution, weather stress, and blood pressure, Am. J. Public Health, 91, 1345-1346, 2001.

Liu, Z., Wang, Y., Gu, D., Zhao, C., Huey, L. G., Stickel, R., Liao, J., Shao, M., Zhu, T., Zeng, L., Amoroso, A., Costabile, F., Chang, C.-C. and Li S.-C.: Summertime photochemistry during CAREBeijing-2007: ROx budgets and O3 formation. Atmos. Chem. Phys., 12, 7737-775, 2012.

Liu, D., Whitehead, J., Alfarra, M. R., Reyes-Villegas, E., Spracklen, D. V., Reddington, C. L., Kong, S., Williams, P. I., Ting, Y.-C., Haslett, S., Taylor, J. W., Flynn, M. J., Morgan, W. T., McFiggans, G., Coe, H. and Allan, J. D.: Black-carbon absorption enhancement in the atmosphere determined by particle mixing state, Nat. Geosci., 10, www.nature.com/naturegeoscience, 2017.

Lozano, R., Naghavi, M., Foreman, K., Lim, S., Shibuya, K., Aboyans, V., Abraham, J., Adair, T., Aggarwal, R., Ahn, S. Y., AlMazroa, M. A., Alvarado, M., Anderson, H. R., Anderson, L. M., Andrews, K. G., Atkinson, C., Baddour, L. M., Barker-Collo, S., Bartels, D. H., Bell, M. L., Benjamin, E. J., Bennett, D., Bhalla, K., Bikbov, B., Abdulhak, A. B., Birbeck, G., Blyth, F., Bolliger, I., Boufous, S., Bucello, C., Burch, M., Burney, P., Carapetis, J., Chen, H., Chou, D., Chugh, S. S., Coffeng, L. E., Colan, S. D., Colquhoun, S., Colson, K. E., Condon, J., Connor, M. D., Cooper, L. T., Corriere, M., Cortinovis, M., de Vaccaro, K. C., Couser, W., Cowie, B. C., Criqui, M. H., Cross, M., Dabhadkar, K. C., Dahodwala, N., De Leo, D., Degenhardt, L., Delossantos, A., Denenberg, J., Des Jarlais, D. C., Dharmaratne, S. D., Dorsey, E. R., Driscoll, T., Duber, H., Ebel, B., Erwin, P. J., Espindola, P., Ezzati, M., Feigin, V., Flaxman, A. D., Forouzanfar, M. H., Fowkes, F. G. R., Franklin, R., Fransen, M., Freeman, M. K., Gabriel, S. E., Gakidou, E., Gaspari, F., Gillum, R. F., Gonzalez-Medina, D., Halasa, Y. A., Haring, D., Harrison, J. E., Havmoeller, R., Hay, R. J., Hoen, B., Hotez, P. J., Hoy, D., Jacobsen, K. H., James, S. L., Jasrasaria, Jayaraman, R., S., Johns, N., Karthikeyan, G., Kassebaum, N., Keren, A., Khoo, J.-P., Knowlton, L. M., Kobusingye, O., Koranteng, A., Krishnamurthi, R., Lipnick, M., Lipshultz, S. E., Ohno, S. L., Mabweijano, J., MacIntyre, M. F., Mallinger, L., March, L., Marks, G. B., Marks, R., Matsumori, A., Matzopoulos, R., Mayosi, B. M., McAnulty, J. H., McDermott, M. M., McGrath, J., Memish, Z. A., Mensah, G. A., Merriman, T. R., Michaud, C., Miller, M., Miller, T. R., Mock, C., Mocumbi, A. O., Mokdad, A. A., Moran, A., Mulholland, K., Nair, M. N., Naldi, L., Narayan, K. M. V., Nasseri, K., Norman, P., O'Donnell, M., Omer, S. B.,. Ortblad, K, Osborne, R., Ozgediz, D., Pahari, B., Pandian, J. D., Rivero, A. P., Padilla, R. P., Perez-Ruiz, F., Perico, N., Phillips, D., Pierce, K., Pope III, C. A., Porrini, E., Pourmalek, F., Raju, M., Ranganathan, D., Rehm, J. T., Rein, D. B., Remuzzi, G., Rivara, F. P., Roberts, T., Rodriguez De León, F., Rosenfeld, L. C., Rushton, L., Sacco, R. L., Salomon, J. A., Sampson, U., Sanman, E., Schwebel, D. C., Segui-Gomez, M., Shepard, D. S., Singh, D., Singleton, J., Sliwa, K., Smith, E., Steer, A., Taylor, J. A., Thomas, B., Tleyjeh, I. M., Towbin, J. A., Truelsen, T., Undurraga, E. A., Venketasubramanian, N., Vijayakumar, L., Vos, T., Wagner, G. R., Wang, M., Wang, W., Watt, K., Weinstock, M. A., Weintraub, R., Wilkinson, J. D., Woolf, A. D., Wulf, S., Yeh, P.-H., Yip, P., Zabetian, A., Zheng, Z.-J., Lopez, A. D. and Murray C. J. L.: Global and regional mortality from 235 causes of death for 20 age groups in 1990 and 2010: a systematic analysis for the Global Burden of Disease Study 2010. The Lancet, 380(9859): 2095-128, 2013.

Lu, K. D., Rohrer, F., Holland, F., Fuchs, H., Bohn, B., Brauers, T., Chang, C. C., Häseler, R., Hu, M., Kita, K., Kondo, Y., Li, X., Lou, S. R., Nehr, S., Shao, M., Zeng, L. M., Wahner, A., Zhang, Y. H., and Hofzumahaus, A.: Observation and modelling of OH and HO2 concentrations in the Pearl River Delta 2006: a missing OH source in a VOC rich atmosphere, Atmos. Chem. Phys., 12, 1541-1569, doi:10.5194/acp-12-1541-2012, 2012.

Lu, K., Guo, S., Tan, Z., Wang, H., Shang, D., Liu, Y., Li, Xin, Wu, Z., Hu, M., Zhang, Y.: Exploring the atmospheric free radical chemistry in China: the self-cleansing capacity and the formation of secondary air pollution, Nat. Sci. Rev., 0: 1–16, doi: 10.1093/nsr/nwy073, 2018.

McDermitt, D., Burba, G., Xu, L., Anderson, T., Komissarov, A., Riensche, B., . . . Hastings, S.: A new low-power, open-path instrument for measuring methane flux by eddy covariance, Appl. Phys. B, 102, 391-405, 10.1007/s00340-010-4307-0, 2011.

McManus, J. B., Zahniser, M. S., Nelson, D. D., Shorter, J. H., Herndon, S. C., Wood, E. C., and Wehr, R.: Application of quantum cascade lasers to high-precision atmospheric trace gas measurements, Opt. Eng., 49, 111124, doi: 10.1117/1.3498782, 2010

Meng, Z., Xu, X., Lin, W., Ge, B., Xie, Y., Song, B., Jia, S., Zhang, R., Peng, W., Wang, Y., Cheng, H., Yang, W., and Zhao, H.: Role of ambient ammonia in particulate ammonium formation at a rural site in the North China Plain, Atmos. Chem. Phys., 18, 167-184, 2018.

Miao, Y., Guo, J., Liu, S., Liu, H., Li, Z., Zhang, W. and Zhai, P.: Classification of summertime synoptic patterns in Beijing and their associations with boundary layer structure affecting aerosol pollution, Atmos. Chem. Phys, 17, 3097-3110, 2017.

Mills, G. P., Hiatt-Gipson, G. D., Bew, S. P., and Reeves, C. E.: Measurement of isoprene nitrates by GCMS, Atmos. Meas. Tech., 9, 4533–4545, 2016.

Molina, L. Madronich, T., S., Gaffney, J. S., Apel, E., de Foy, B., Fast, J., Ferrare, R., Herndon, S., Jimenez, J. L., Lamb, B., Osornio-Vargas, A. R., Russell, P., Schauer, J. J., Stevens, P. S., Volkamer R. and Zavala M.: An overview of the MILAGRO 2006 Campaign: Mexico City emissions and their transport and transformation, Atmos. Chem. Phys., 10, 8697-8760, 2010.

Moore, E., Chatzidiakou, L., Jones, R. L., Smeeth, L., Beevers, S., Kelly, F. J., Quint, J. K., Barratt, B.: Linking e-health records, patientreported symptoms and environmental exposure data to characterise and model COPD exacerbations: protocol for the COPE study, BMJ Open, 6, e011330,10.1136/bmjopen-2016-011330, 2016.

Nemitz, E., Hargreaves, K. J., McDonald, A.G., Dorsey, J. R., and Fowler, D.: Micrometeorological measurements of the urban heat budget and CO_2 emissions on a city scale, Environ. Sci. Technol., 36, 3139-3146, 2002.

Nemitz, E., Jimenez, J. L., Huffman, J. A., Ulbrich, I. M., Canagaratna, M. R., Worsnop, D. R. and Guenther, A. B.: An eddy-covariance system for the measurement of surface/atmosphere exchange fluxes of submicron aerosol chemical species - first application above an urban area, Aerosol Sci. Technol., 42, 636-657, 2008.

OECD, 2016. The economic consequences of outdoor air pollution - policy highlights. OECD Publishing, Paris, https://doi.org/10.1787/9789264257474-en.

Pang, X., Lewis, A. C., Rickard, A. R., Baeza-Romero, M. T., Adams, T. J., Ball, S. M., Daniels, M. J. S., Goodall, I. C. A., Monks, P. S., Peppe, S., Ródenas García, M., Sánchez, P., and Muñoz A.: A smog chamber comparison of a microfluidic derivatisation measurement of gas-phase glyoxal and methylglyoxal with other analytical techniques, Atmos. Meas. Tech., 7, 373-389, 2014.

Palmer, P.I., Jacob, D.J., Fiore, A.M., Martin, R.V., Chance, K., Kurosu,T.P., Mapping isoprene emissions over North America using formaldehyde column observations from space. J. Geophys. Res.-Atmos., 108, D6, doi: 10.1029/2002JD002153, 2003.

Petäjä, T., Mordas, G., Manninen, H., Aalto, P. P., Hämeri, K., and Kulmala, M.: Detection Efficiency of a Water-Based TSI Condensation Particle Counter 3785, Aerosol Science and Technology, 40, 1090-1097, doi:10.1080/02786820600979139, 2006.

Philipp, A., Bartholy, J., Erpicum, M., Esteban, P., Fettweis, X., James, P., Jourdain, S., Kreienkamp, F., Krennert, T., Lykoudis, S., Michalides, S. C., Pianko-Kluczynska, K., Post, P., Álvarez, D. R., Schiemann, R., Spekat, A. and Tymvios, F. S.: Cost733cat – A database of weather and circulation type classifications, Phys. Chem. Earth, Parts A/B/C, 35(9–12), 360-373, 2010.

Philipp, A., Beck, C., Huth, R. and Jacobeit, J.: Development and comparison of circulation type classifications using the COST 733 dataset and software, Int. J. Climatol., 36(7), 2673-2691, 2016.

Popoola, O. A., Carruthers, D., Lad, C., Bright, V. B., Mead, I.M., Stettler, M., Saffell, J. and Jones, R.L.: The use of networks of low cost air quality sensors to quantify air quality in urban settings, Atmos. Environ., in review, 2018.

Shi, J.P., Harrison, R.M., Brear, F.: Particle size distribution from a modern heavy duty diesel engine, Sci. Total Environ., 235, 305-317, 1999.

Sloan, C. D., Philipp, T. J., Bradshaw, R. K., Chronister, S., Bradford Barber, W., and Johnston, J. D.: Applications of GPS-tracked personal and fixed-location PM2.5 continuous exposure monitoring, JAWMA, 66, 53-65, 2016.

Smith, K. R., Edwards, P. M., Evans, M. J., Lee, J. D., Shaw, M. D., Squires, F., Wilde, S., and Lewis, A. C.: Clustering approaches to improve the performance of low cost air pollution sensors, Faraday Discuss., 200, 621, 2017.

Stone, D., Whalley, L. K., Ingham, T., Edwards, P. M., Crye,r D. R., Brumby, C. A., Seakins, P. W., Heard, D. E.: Measurement of OH reactivity by laser flash photolysis coupled with laser-induced fluorescence spectroscopy, Atmos. Measure. Tech., 9, 2827-2844, 2016.

Storer, M., Salmond, J., Dirks, K. N., Kingham, S., and Epton M.: Mobile selected ion flow tube mass spectrometry (SIFT-MS) devices and their use for pollution exposure monitoring in breath and ambient air–pilot study, J. Breath Res., 8, 037106 (7pp), doi:10.1088/1752-7155/8/3/037106, 2014.

Sun, Y. L., Wang, Z., Dong, H., Yang, T., Li, J., Pan, X., Chen, P., and Jayne, J. T.: Characterization of summer organic and inorganic aerosols in Beijing, China with an Aerosol Chemical Speciation Monitor, Atmos. Environ., 51, 250-259, 2012.

Sun, Y., Du, W., Fu, P., Wang, Q., Li, J., Ge, X., Zhang, Q., Zhu, C., Ren, L., Xu, W., Zhao, J., Han, T., Worsnop, D., and Wang, Z.: Primary and secondary aerosols in Beijing in winter: sources, variations and processes, Atmos. Chem. Phys., 16, 8309-8329, 2016.

Taiwo, A. M., Beddows, D. C. S., Calzolai, G., Harrison, R. M., Lucarelli, F., Nava, S., Shi, Z., Valli, G., and Vecchi, R.: Receptor modelling of airborne particulate matter in the vicinity of a major steelworks site, Sci. Tot. Environ., 490, 488-500, 2014.

Tan, Z., Fuchs, H., Lu, K., Hofzumahaus, A., Bohn, B., Broch, S., Dong, H., Gomm, S., Häseler, R., He, L., Holland, F., Li, X., Liu, Y., Lu, S., Rohrer, F., Shao, M., Wang, B., Wang, M., Wu, Y., Zeng, L., Zhang, Y., Wahner, A., and Zhang, Y.: Radical chemistry at a rural site (Wangdu) in the North China Plain: observation and model calculations of OH, HO2 and RO2 radicals, Atmos. Chem. Phys., 17, 663-690, 2017.

Tao, S., Ru, M. Y., Du, W., Zhu, X., Zhong, Q. R., Li, B. G., Shen, G. F., Pan, X. L., Meng, W. J., Chen, Y. L., Shen, H. Z., Lin, N., Su, S., Zhuo, S. J., Huang, T. B., Xu, Y., Yun, X., Liu, J. F., Wang, X. L., Liu, W. X., Chen, H. F., Zhu, D. Q.: Quantifying the Rural Residential Energy Transition in China from 1992 to 2012 through a Representative National Survey, Nat. Energy, 3, 567-573, 2018.

Tveito, O. E., and Huth, R.: Circulation-type classifications in Europe: results of the COST 733 Action, Int. J. Climatol., 36, 2671-2672, 2016.

Vanhanen, J., Mikkilä, J., Lehtipalo, K., Sipilä, M., Manninen, H. E., Siivola, E., Petäjä, T., and Kulmala, M.: Particle size magnifier for nano-CN detection, Aerosol Sci. Tech., 45, 533-542, 2011.

Vaughan, A. R., Lee, J. D., Misztal, P. K., Metzger, S., Shaw, M. D., Lewis, A. C., Purvis, R. M., Carslaw, D. C., Goldstein, A. H., Hewitt, C. N., Davison, B., Beeversh, S. D. and Karl, T. G.: Spatially resolved flux measurements of NO_x from London suggest significantly higher emissions than predicted by inventories, Faraday Discuss., 189, 455, 2016.

Wang, M., Zhu, T., Zheng, J., Y. Zhang, R., Zhang, S. Q., Xie, X. X., Han, Y. Q., and Li, Y.: Use of a mobile laboratory to evaluate changes in on-road air pollutants during the Beijing 2008 Summer Olympics, Atmos. Chem. Phys., 9, 8247-8263, 2009.

Wang, M., Shao, M., Chen, W., Lu, S., Liu, Y., Yuan, B., Zhang, Q., Zhang, Q., Chang, C.-C., Wang, B., Zeng, L., Hu, M., Yang, Y., and Li, Y.: Trends of non-methane hydrocarbons (NMHC) emissions in Beijing during 2002-2013, Atmos. Chem. Phys., 15, 1489-1502, 2015a.

Wang, Q., Sun, Y., Jiang, Q., Du, W., Sun, C., Fu, P., and Wang, Z.: Chemical composition of aerosol particles and light extinction apportionment before and during the heating season in Beijing, China, J. Geophys. Res., 120, 12708-12722, 10.1002/2015JD023871, 2015b.

Wang, J., Zhang, Q., Chen, M.-D., Collier, S., Zhou, S., Ge, X., Xu, J., Shi, J., Xie, C., Hu, J., Ge, S., Sun, Y., and Coe, H.: First chemical characterization of refractory black carbon aerosols and associated coatings over the Tibetan Plateau (4730 m a.s.l), Environ. Sci. Technol., 51, 14072-14082, 2017a.

Wang, Y., Zhang, F., Li, Z., Tan, H., Xu, H., Ren, J., Zhao, J., Du, W., and Sun, Y.: Enhanced hydrophobicity and volatility of submicron aerosols under severe emission control conditions in Beijing, Atmos. Chem. Phys., 17, 5239-5251, 2017b.

Wang, W., Shao, L., Xing, J., Li, J., Chang, L. and Li, W.: Physicochemical characteristics of individual aerosol particles during the 2015 China victory day parade in Beijing, Atmosphere, 9, 40; doi:10.3390/atmos9020040, 2018.

Whalley, L. K., Furneaux, K. L., Goddard, A., Lee, J. D., Mahajan, A., Oetjen, H., Read, K. A., Kaaden, N., Carpenter, L. J., Lewis, A. C., Plane, J. M. C., Saltzman, E. S., Wiedensohler, A., and Heard D. E.: The chemistry of OH and HO_2 radicals in the boundary layer over the tropical Atlantic Ocean, Atmos. Chem. Phys., 10, 1555-1576, 2010.

WHO: Ambient air pollution: a global assessment of exposure and burden of disease. ISBN 978 92 151135 3, 2016a.

WHO: Burden of disease from joint household and ambient air pollution for 2012. http://www.who.int/phe/health_topics/outdoorair/databases/AP_jointeffect_methods_Nov2016.pdf?ua=1, 2016b.

Wragg, F. P. H., Fuller, S. J., Freshwater, R., Green, D. C., Kelly, F. J., and Kalberer M.: An automated online instrument to quantify aerosol-bound reactive oxygen species (ROS) for ambient measurement and health-relevant aerosol studies, Atmos. Meas. Tech., 9, 4891-4900, 2016.

Wu, Z. J., Poulain, L., Henning, S., Dieckmann, K., Birmili, W., Merkel, M., van Pinxteren, D., Spindler, G., Müller, K., Stratmann, F., Herrmann, H., and Wiedensohler, A.: Relating particle hygroscopicity and CCN activity to chemical composition during the HCCT-2010 field campaign, Atmos. Chem. Phys., 13, 7983-7996, 2013.

Wu, Z. J., Zheng, J., Shang, D. J., Du, Z. F., Wu, Y. S., Zeng, L. M., Wiedensohler, A., and Hu, M.: Particle hygroscopicity and its link to chemical composition in the urban atmosphere of Beijing, China, during summertime, Atmos. Chem. Phys., 16, 1123-1138, 2016.

Wu, J., Li, G., Cao, J., Bei, N., Wang, Y., Feng, T., Huang, R., Liu, S., Zhang, Q. and Tie, X.: Contributions of trans-boundary transport to summertime air quality in Beijing, China, Atmos. Chem. Phys., 17, 2035-2051, 2017.

Xia, Y., Guan, D., Jiang, X., Peng, L., Schroeder, H., Zhan, Q.: Assessment of socioeconomic costs to China's air pollution. Atmos. Environ. 139, 147-156, 2016.

Xie, C., Xu, W., Wang, J., Wang, Q., Liu, D., Tang, G., Chen, P., Du, W., Zhao, J., Zhang, Y., Zhou, W., Han, T., Bian, Q., Li, J., Fu, P., Wang, Z., Ge, X., Allan, J., Coe, H., and Sun, Y.: Vertical characterization of aerosol optical properties and brown carbon in winter in urban Beijing, China, Atmospheric Chemistry and Physics Discussions, 1-28, 10.5194/acp-2018-788, 2018.

Yang, G., Wang, Y., Zeng, Y., Gao, G. F., Liang, X., Zhou, M., Wan, X., Yu, S., Jiang, Y., Naghavi, M., Vos, T., Wang, H., Lopez, A. D., Murray, C. J. L.: Rapid health transition in China, 1990-2010: findings from the Global Burden of Disease Study 2010, The Lancet, 381, 1987-2015, 2013.

Yu, J., Yan, C., Liu, Y., Li, X., Zhou, T., Zheng, M.: Potassium: A Tracer for Biomass Burning in Beijing? Aerosol Air Qual. Res., 18, 2447-2459, 2018.

Yue, S., Ren, H., Fan, S., Sun, Y., Wang, Z. and Fu P.: Springtime precipitation effects on the abundance of fluorescent biological aerosol particles and HULIS in Beijing, Sci. Rep., 6, 29618, 10.1038/srep29618, 2016.

Zhang, Q., Streets, D. G., Carmichael, G. R., He, K. B., Huo, H., Kannari, A., Klimont, Z., Park, I. S., Reddy, S., Fu, J. S., Chen, D., Duan, L., Lei, Y., Wang, L. T., and Yao, Z. L.: Asian emissions in 2006 for the NASA INTEX-B mission, Atmos. Chem. Phys., 9, 5131-5153, 2009.

Zhang, J. B., Xu, Z., Yang, G., and Wang, B.: Peroxyacetyl nitrate (PAN) and peroxypropionyl nitrate (PPN) in urban and suburban atmospheres of Beijing, China, Atmos. Chem. Phys. Discuss., 11, 8173-8206, 2011.

Zhang, J. P., Zhu, T., Zhang, Q. H., Li, C. C., Shu, H. L., Ying, Y., Dai, Z. P., Wang, X., Liu, X. Y., Liang, A. M., Shen, H. X. and Yi, B. Q.: The impact of circulation patterns on regional transport pathways and air quality over Beijing and its surroundings, Atmos. Chem. Phys., 12, 5031-5053, 2012.

Zhang, Q., Jiang, X., Tong, D., Davis, S. J., Zhao, H., Geng, G., Feng, T., Zheng, B., Lu, Z., Streets, D. G., Ni, R., Brauer, M., van Donkelaar, A., Martin, R. V., Huo, H., Liu, Z., Pan, D., Kan, H., Yan, Y., Lin, J., He, K.and Guan, D.: Transboundary health impacts of transported global air pollution and international trade, Nature 543, 705-709, 2017a.

Zhang, Y., Ren, H., Sun, Y., Cao, F., Chang, Y., Liu, S., Lee, X., Agrios, K., Kawamura, K., Liu, D., Ren, L., Du, W., Wang, Z., Prevot, A. S. H., Szidat, S., and Fu, P.: High contribution of non-fossil sources to sub-micron organic aerosols in Beijing, China, Environ. Sci. Technol., 2017b.

Zhao, W., Kawamura, K., Yue, S., Wei, L., Ren, H., Yan, Y., Kang, M., Li, L., Ren, L., Lai, S., Li, J., Sun, Y., Wang, Z., and Fu P.: Molecular distribution and compound-specific stable carbon isotopic composition of dicarboxylic acids, oxocarboxylic acids and α-dicarbonyls in $PM_{2.5}$ from Beijing, China, Atmos. Chem. Phys., 18, 2749–2767, 2018.

Zhou, W., Zhao, J., Ouyang, B., Mehra, A., Xu, W., Wang, Y., Bannan, T. J., Worrall, S. D., Priestley, M., Bacak, A., Chen, Q., Xie, C., Wang, Q., Wang, J., Du, W., Zhang, Y., Ge, X., Ye, P., Lee, J. D., Fu, P., Wang, Z., Worsnop, D., Jones, R., Percival, C. J., Coe, H., and Sun, Y.: Production of N_2O_5 and $ClNO_2$ in summer in urban Beijing, China, Atmos. Chem. Phys., 18, 2018.

Atmos. Chem. Phys. Discuss., https://doi.org/10.5194/acp-2018-922
Manuscript under review for journal Atmos. Chem. Phys.
Discussion started: 15 October 2018

Atmospheric Chemistry and Physics Discussions

TABLE LEGENDS:

Table 1: Overview of measurements in APHH-Beijing at the urban site.

Table 2: Haze periods during the summer and winter campaign periods.

Table 3: Overview of measurements at the Pinggu site.

Table 4: Average air quality variables at IAP, Pinggu and 12 national monitoring sites (12N) during the field campaigns (10 November – 11 December 2016; and 21 May – 22 Jun 2017). The 12 national sites five-year mean concentrations for same times of the years (12N -5Y) and for the same time of the year (campaign period) (12N-campaign). Data are mean ± s.d. (range).

Table 5: Mean and standard deviation (sd) of climatological conditions in Beijing for each circulation type (CT) for 1988-20 17 from Era Interim data with frequency of the CT during the W (winter) and S (summer) campaigns (% of 6 h periods (p)) compared to A- long- term 1988-2017.

FIGURE LEGENDS

Figure 1: Study area topography (source: googlemap) of Beijing / Tianjing / Hebei region (a) with the rectangle showing enlarged study area; locations of measurement sites (Institute of Atmospheric Physics (IAP)– urban Beijing, Pinggu – rural Beijing; and Gucheng – upwind site in Hebei province), SNAQ box sites (red symbols) and the 12 national air quality monitoring stations (G1 to G12, blue symbols) (b); locations of the 9 containers at IAP (c) – instrumentation at each container is shown in Table 1. The shaded area shows the Beijing buildup area. (Source: a and b - Goggle Map topographic background imagery; c – taken by Siyao Yue from IAP).

G1: Wangshouxigong; G2: Dingling; G3: Dongsi; G4: Tiantan; G5: Nongzhanguan; G6: Guanyuan; G7: Haidianquwanliu; G8: Shunyxicheng; G9: Huairouzhen; G10:Changpingzhen; G11: Aotizhongxin (Olympic Park); G12: Gucheng. Categories: Urban: G1, G3, G4, G5, G6, G7, G8, G11, G12; Suburban: G9, G10; Rural: G2.

Figure 2: Time-series of air quality variables at the urban and rural sites during the winter campaign; Five haze events are indicated (shading).

Figure 3: Diurnal patterns of gaseous pollutants normalized by average concentrations at IAP during winter and summer campaigns. Line shows the mean concentrations and shaded area as 95% confidence interval in the difference in mean concentrations

Figure 4: Air pollutants concentration (colour) with wind direction (angle) and wind speed (m s^{-1}) at IAP during the winter and summer campaigns. Data are hourly in time resolution and were from 10 November to 11 December 2016 (winter) and 21 May to 22 June 2017 (summer). The colour scale is for “weighted.mean” where the mean wind speed/direction bin is multiplied by the bin frequency and divided by total frequency.

Atmos. Chem. Phys. Discuss., https://doi.org/10.5194/acp-2018-922
Manuscript under review for journal Atmos. Chem. Phys.
Discussion started: 15 October 2018

Atmospheric Chemistry and Physics
Discussions

Figure 5: Time series of CO_2, CO, NO, O_x (NO_2+O_3) and wind speed at six heights (colour) measured with SNAQ boxes on the IAP tower during the winter intensive field campaign.

Figure 6: Hourly $PM_{2.5}$ mass concentrations versus visibility (at the Beijing Capital Airport) during the winter campaign. Data source: visibility downloaded using R-"worldmet" package: date of last access: 27/02/2018).

Figure 7: Time-series of air quality variables at the urban and rural sites during the summer campaign. Two minor haze events are indicated (shading).

Figure 8: Correlations between the air quality at IAP, PQ and 12 monitoring station around Beijing. Stations G1-G12 (Figure 2) are labelled 01-12, PG = Pinggu.

Figure 9: Spatial distribution of hourly mean concentration of $PM_{2.5}$ in Beijing during two sampling campaigns.

Figure 10: Hourly $PM_{2.5}$ at IAP (roof of a two storied building) and the neighbouring Olympic park national air quality monitoring station during the winter and summer intensive field campaigns.

Figure 11: ERA-Interim (1988-2017) average 925 hPa geopotential with 10 m horizontal wind vector for 11 circulation types classified for Beijing (municipal boundary thin solid line) surroundings (103-129° E, 31 - 49° N) determined with the SANDRA method (COST733 class software). Frequency of occurrence is given in cluster caption. For discussion of conditions associated with each CT see section 6.1.

Figure 12: Time series of circulation types (CTs) during the two field campaigns: (a) winter and (b) summer. The 11 CTs are shown in Figure 11. See text for more description.

Figure 13: Analysis by circulation type (CT; Sect. 0) of: (a) daily maximum mixed layer height (MLH) determined from ALC observations at IAP between November 2016 – June 2017 (analysis method, Kotthaus and Grimmond, 2018b); concentration of (b) $PM_{2.5}$ and (c) O_3 at at the Olympic Park (i.e. Aotizhongxin) in 2013-2017 from the national air quality network; occurrence of CTs in (d) 1988-2017 and (e) Oct 2016 – Sept 2017; (f) anomaly of CT frequency during Oct 2016 – Sept 2017 compared to 30 y climatology; and (g) anomaly of $PM_{2.5}$ and O_3 during Oct 2016 – Sept 2017 compared to 5 y (2013-2017) average (same data as in b, c).

Figure 14: Beijing wind roses: (a, b, d, e) ERA-Interim 10 m horizontal wind (40° N, 116.5° E) and (c, f) sonic anemometer (Table 1) at IAP 320 m agl for (a) 5 November – 10 December in 1988-2017, (d) 15 May – 22 June in 1988-2017, (b, c) 5 November – 10 December 2016, and (e, f) 15 May – 22 June 2017.

Figure 15: Hourly meteorological variables measured at 120 m during the (a) winter and (b) summer campaigns. The shaded areas highlighted the haze periods (Table 3, Figures 2 and 7).

Figure 16: Frequency distribution of $PM_{2.5}$ in Beijing over the winter (left) and summer (right) campaign periods from the NAQPMS model compared with those from the same periods over the past five years under the same emission conditions.

Table 1: Overview of measurements in APHH-Beijing at the urban site.

	Instrument	Measurements	Institute	References
Container 2	FAGE	OH (Chem and Wave)^{X}, HO_2, RO_2	Leeds	Whalley et al. (2010)
	OH reactivity	OH reactivity	Leeds	Stone et al. (2016)
	Spectral radiometer	Photolysis rates	Leeds	Bohn et al. (2016)
	Filter radiometer	$J(O^1D)$	Leeds	Bohn et al. (2016)
	Dew point hygrometer	Water vapour	Leeds	Whalley et al. (2010)
	Davis met station	Wind speed, direction, temp, RH, pressure	Leeds	
	Vaisala CL31 ALC Ceilometer $^{+}$	Cloud-base height, mixing height, attenuated backscatter profiles	Reading	Kotthaus and Grimmond (2018a)
	Personal air monitors (PAMS)	CO, NO, NO_2, PM_1, PM_{10}, $PM_{2.5}$	Cambridge	Moore et al. (2016)
	MicroPEMs	Personal PM exposure	IOM	Sloan et al. 2015
Container 2	DC-GC-FID	C2-C7 VOCs and oVOCs	York	Hopkins et al. (2011)
	GCxGC FID	C6 - C13 VOCs and oVOCs	York	Dunmore et al. (2015)
	TEI 42i	NO	Birmingham	
	Teledyne CAPS	NO_2	York	
	TEI 42c	Total NO_y	York	
	TEI 49i	O_3	York	
	TEI 43i	SO_2	York	
	Sensor box	CO	York	Smith et al. (2017)
	BBCEAS	HONO, NO_3, N_2O_5	Cambridge	Le Breton et al. (2014)
Container 3	LOPAP	HONO	Birmingham	Crilley et al. (2016)
	LIF HCHO	HCHO	Leeds	Cryer et al. 2016
	LOPAP	HONO	IC-CAS	Zhang et al. (2018)
	GC-MS	Organic nitrates	East Anglia	Mills et al. (2016)
	ROS online analyser	Reactive Oxygen Species	Cambridge	Wragg et al. (2016)
Container 4*	FAGE	OH (wave)^{x}, HO_2	Peking	Lu et al., 2012
	FAGE	OH (chem)^{x}	Peking	Tan et al., 2017
	TEI 42i	NO	Peking	Tan et al., 2017
	Teledyne CAPS	NO2	Peking	
	TEI 42c with Moly converter	NO_2	Peking	
	TEI 49i	O_3	Peking	
	TEI	CO	Peking	
	Spectral radiometer	Photolysis rates	Peking	
	GC-ECD	PAN	Peking	Zhang et al., 2011
	GC-MS	VOCs	Peking	Wang et al., 2015a

Atmos. Chem. Phys. Discuss., https://doi.org/10.5194/acp-2018-922
Manuscript under review for journal Atmos. Chem. Phys.
Discussion started: 15 October 2018

Container 5[*]	H-TDMA/V-TDMA	Hygroscopicity/volatility	Peking	Wu et al., 2013
	SMPS+APS	Particle Number size distribution	Peking	Wu et al., 2016
	Particle size magnifier	Size distribution of < 3nm particles	Peking	Vanhanen et al., 2011
	IGAC-IC	Water-soluble ions	Peking	Yu et al. (2018)
	Xact	Metal	Peking	Yu et al. (2018)
	Sunset OC/EC	EC/OC	Peking	Zhang et al. (2017b)
Container 6	IBBCEAS	HONO, NO_2	AIOFM	Duan et al. (2018)
	CRDS	NO_3 and N_2O_5	AIOFM	Li et al. (2018)
	Nitrate Api-TOF-CIMS	Organics, clusters (HOMs)	Birmingham	Junninen et al. (2010)
	SMPS	Particle size distribution	Birmingham	Shi et al. (1999)
	Particle size magnifier	Size distribution of < 3 nm particles	Birmingham	Vanhanen et al. (2011)
Container 7	Fast NO_x	NO_x fluxes	York	Vaughan et al. (2016)
	AL5002 CO analyser	CO fluxes	York	Gerbig et al. (1999)
	HR-TOF-AMS	Fluxes of PM_1 non-refractory (NR) species	CEH	Nemitz et al. (2008)
	SP2	BC fluxes	Manchester	Liu et al. (2017)
	PTR-TOF-MS	VOC fluxes	GIG Lancaster	Huang et al. (2016)
	SYFT-MS Voice 200 Ultra	VOC fluxes	York	Storer et al. (2014)
Container 8	SMPS3968-APS3321	Particle number size distribution	BNU	Du et al. (2017)
	H/V TDMA	Particle hygroscopicity	BNU	Wang et al. (2017b)
	CCNC-100	CCN	BNU	Wang et al. (2017b)
	PAX (870nm)	Extinction & absorption coefficient	IAP	Xie et al. (2018)
	Ammonia analyzer	NH_3	IAP	Meng et al. (2018)
	Sunset OC/EC analyzer	Online OC/EC	IAP	Zhang et al. (2017b)
Container 9	Iodide FIGAERO-TOF-CIMS	Particle and gas phase molar molecule	Manchester	Le Breton et al. (2018)
	CPMA-SP2	Black carbon mass and mixing state	Manchester	Liu et al. (2017)
	Micro reactor	oVOCs	York	Pang et al. (2014)
Tower ~100 m	QCL NH_3	Ammonia fluxes	CEH	McManus et al. (2010)
	IRGA LiCOR-7500	CO_2 / H_2O flux	CEH	McDermitt et al. (2011)
	DMT UHSAS	Size resolved particle flux (0.06-1 µm)	CEH	Deventer et al. (2015)

	TSI APS3021	Size-resolved particle flux (0.5-25 µm)	CEH	Nemitz et al. (2002)
	TSI CPC3785	Total particle number flux	CEH	Petäjä et al. (2006)
	ROFI	O_3 flux	CEH	Coyle et al. (2009)
	Sonic anemometer R3-50	Turbulence, sensible heat flux	CEH	Högström and Smedman (2004)
	WXT530 weather station	T, P, RH, wind speed & direction, precipitation	CEH	
	2B O_3 analyser	O_3 concentration	CEH	Johnson et al. (2014)
Tower ~120 m	High-vol sampler	$PM_{2.5}$ filter samples	IAP	
	Anderson sampler	Size-resolved PM samples	IAP	
Tower ~260 m	High-vol sampler	$PM_{2.5}$ filter samples	IAP	
	Anderson sampler	Size- resolved PM samples	IAP	
	ACSM	NR PM_1 species	IAP	Sun et al. (2012)
	CAPS-PM-$_{Ext}$ (630nm)	Extinction	IAP	Wang et al. (2015b)
	SMPS 3938	Particle Number size distribution	IAP	Du et al. (2017)
	Gas analyser	CO, O_3 and SO_2	IAP	Zhou et al. (2018)
	Aethalometer AE33	Black carbon	IAP	Xie et al. (2018)
	Single particle sampler	Individual particles	CUMTB	Wang et al. (2018)
Tower and tower basket measurements	SNAQ boxes (x 6 at different heights)	CO, NO, NO_2, SO_2, PM_1, PM_{10}, $PM_{2.5}$	Cambridge	Popoola et al. (2018)
	LOPAP	HONO (3 min avg)	Birmingham	Crilley et al. (2016)
	Spectral radiometer	Photolysis rates	Leeds	Bohn et al. (2016)
	SNAQ	CO, NO, NO_2, SO_2, PM_1, PM_{10}, $PM_{2.5}$	Cambridge	Popoola et al. (2018)
	WIBS	Fluorescent biological aerosol particles (FBAP)	IAP	Yue et al. (2016)
	AE33	BC	IAP	Xie et al. (2018)
	Los Gatos NH_3 Analyzer	NH_3	IAP	Meng et al. (2018)
	PAX	Light scattering / absorption	IAP	Xie et al. (2018)
IAP groun	High-Vol sampler	*$PM_{2.5}$* filter samples	Peking	

	4-channel sampler	*$PM_{2.5}$ filter samples*	Peking	
	High Vol sampler	*High time resolution $PM_{2.5}$* filter samples	York	
IAP roof/lab	FDMS+Thermo Scientific 1405-DF	Online $PM_{2.5}$ mass conc.	IAP	
	Partisol sampler	$PM_{2.5}$ + $PM_{2.5-10}$	Birmingham	Taiwo et al. (2014)
	Streaker sampler	Hourly elements in $PM_{2.5}$ and $PM_{2.5-10}$	Birmingham	Taiwo et al. (2014)
	Digitel High Vol	$PM_{2.5}$ daily	IAP	
	Digitel High Vol	PM_1 - 3 hourly	IAP	
	Andersen sampler	Size resolved PM	IAP	
	WIBS	Fluorescent biological particles	IAP	Yue et al. (2016)
	CAPS-NO_2	NO_2	IAP	Ge et al. (2013)
	Aethalometer AE33	Black carbon	IAP	Xie et al. (2018)
	CAPS-PM_{SSA} (630nm)	Extinction, Scattering	IAP	Han et al. (2017)
	HR-ToF-AMS	NR-PM species	IAP	Sun et al. (2016)
	SP-AMS	Refractory BC and coated aerosol composition		Wang et al. (2017a)
	Iodide FIGAERO-ToF-CIMS	Particle and gas phase molar molecule	IAP	Zhou et al. (2018)
	Single particle sampler	Individual particles	CUMTB	Wang et al. (2018)

Institution names: AIOFM = Anhui Institute of Fine Optics and Mechanics; BNU = Beijing Normal University; CEH = Centre for Ecology and Hydrology; CUMTB = China University of Mining and Technology (Beijing); GIG = Guangzhou Institute of Geochemistry, Chinese Academy of Sciences; NUIST = Nanjing University of Information Science &Technology; IC-CAS = Institute of Chemistry, Chinese Academy of Sciences

[+] Deployment of instruments both campaigns unless: 10/11/2016 to 25/6/2017

[*] Winter campaign only

[X] OH wave and OH chem refer to the method used to obtain the background signal for the FAGE instruments which are equipped with a scavenger inlet

Table 2: Haze periods during the summer and winter campaign periods.

Event	Time	$PM_{2.5}$ (μg m^{-3})	Visibility (km)
Winter Haze Event 1	11/08 21:00- 11/10 16:00	158 (79 - 229)	4.1 (2.3-8)
Winter Haze Event 2	11/15 21:00- 11/19 08:00	143 (56 - 244)	4.2(0.6-8)
Winter Haze Event 3	11/24 12:00- 11/27 02:00	210 (68-363)	4.2(1.5-8)
Winter Haze Event 4	12/02 16:00- 12/05 02:00	239 (58 -530)	3.9(0.9-8)
Winter Haze Event 5	12/06 09:00- 12/08 10:00	144 (64 -229)	4.6(2.2-8)
Summer Haze Event 1	27/05 12:00 -28/05 13:00	107(62- 163)	6.8(4.5-9)
Summer Haze Event 2	17/06 09:00-18/06 17:00	90.5(60-153.3)	9.3(7-13)

Note: data in parentheses show the range

Atmos. Chem. Phys. Discuss., https://doi.org/10.5194/acp-2018-922
Manuscript under review for journal Atmos. Chem. Phys.
Discussion started: 15 October 2018

Table 3: Overview of measurements at the Pinggu site.

Instruments	**Measurements**	**Insitutue**	**Reference**
Thermo gas analysers	$NO_x/SO_2/CO/O_3$	Peking	Liang et al., 2017
BAM 1020	$PM_{2.5}$ mass concentration	Peking	Liang et al., 2017
High vol sampler	$PM_{2.5}$ samples	IAP	Zhao et al., 2018
Medium vol sampler	$PM_{2.5}$ samples	IAP	Zhao et al., 2018
Low vol Andersen sampler	Size resolved PM samples	IAP	Zhao et al., 2018
Partisol sampler	$PM_{2.5}$ samples	Birmingham	Taiwo et al. (2014)
Streaker sampler	Hourly elements in $PM_{2.5}$ and $PM_{2.5-10}$	Birmingham	Taiwo et al. (2014)
High vol sampler	Filters of $PM_{2.5}$; high time resolution	Birmingham	
Four Channel sampler	$PM_{2.5}$ samples	Peking	Liang et al., 2017
Thermo MAAP	Online Black Carbon	Peking	Lin et al., 2011
Sunset OC/EC analyzer	Online OC/EC	Peking	Han et al., 2014
Xact	Hourly metals	Peking	Yu et al. (2018)
TOF-ACSM	NR-chemical composition (summer)	Peking	Sun et al., 2012
Thermo Metone	Meteorological parameters	Peking	Liang et al., 2017
SNAQ	Meteorological parameters	Cambridge	Popoola et al. (2018)
SP-AMS	Individual particle composition	CQIGIT	Chen et al. (2017)
SMPS	Size distribution	Tsinghua	Wang et al., 2009
ACSM	NR-chemical composition (winter)	Tsinghua	Li et al. (2016)

CQIGIT = Chongqing Institute of Green and Intelligence Technology, Chinese Academy of Sciences

Table 4: Average air quality variables at IAP, Pinggu and 12 national monitoring sites (12N) during the field campaigns (10 Novemberember – 11 December 2016; and 21 May – 22 June 2017). The 12 national sites five-year mean concentrations for same times of the years (12N -5Y) and for the same time of the year (campaign period) (12N-campaign). Data are mean ± s.d. (range).

Pollutant[1]	**Winter** *(10 Nov-11 Dec 2016)*				**Summer** *(21 May-22 June 2017)*			
	IAP	PG	12N-5Y	12N - campaign	IAP	PG	12N-5Y	12N-campaign
$PM_{2.5}$ [2]	91.2 ± 63.7 (10.3-239.9)	99.7 ± 77.8 (13.3-294.3)	84.01 ± 89.1 (3.2-593.3)	95.3 ± 79.6 (4.7-408.8)	31.4 ± 14.7 (12.2-78.8)	27.8 ± 13.3 (10.6-70.3)	58.7 ± 40.0 (4.2-250.3)	41.7 ± 22.3 (8.9-134.1)
PM_{10} [2]	130.6 ± 87.0 (20.0-329.2)	121.9 ± 80.4 (10.4-312.1)	112.8 ± 102.2 (5-662.0)	134.5 ± 100.4 (6.0-550.1)	74.9 ± 29.3 (22.5-164.6)	62.9 ± 29.3 (15.1-141.9)	94.6 ± 52.7 (5.0-463.2)	81.9 ± 37.1 (6.0-277.8)
NO_2	69.7 ± 33.3 (10.2-167.3)	46.4 ± 25.5 (2.3-132.4)	57.7 ± 33.9 (3.9-166.4)	66.4 ± 31.3 (7.3-156.6)	41.3 ± 23.5 (9.2-142.9)	29.3 ± 10.3 (9.3-84.0)	40.6 ± 17.9 (8.1-132.4)	37.6 ± 16.2 (12.5-92.8)
SO_2	14.9 ± 11.1 (0.1-50.8)	15.4 ± 6.7 (6.2-44.4)	16.6 ± 16.2 (1.4-112.0)	14.2 ± 9.4 (2.1-51.4)	6.3 ± 6.8 (0.1-38.2)	8.9 ± 4.7 (4.2-41.2)	10.1 ± 10.6 (1.8-82.3)	7.4 ± 6.6 (1.8-64.5)
CO [2]	1.53 ± 1.02 (0.7-5.0)	1.47 ± 1.17 (0.1-6.9)	1.65 ± 1.38 (0.1-9.6)	1.86 ± 1.17 (0.3-5.7)	0.61 ± 0.32 (0.1-2.5)	0.52 ± 0.29 (0.1-2.3)	0.93 ± 0.74 (0.2-8.7)	0.74 ± 0.33 (0.2-2.5)
O_3	16.4 ± 17.0 (0.3-63.3)	22.3 ± 22.2 (2.9-78.0)	21.8 ± 20.5 (1.0-72.9)	17.5 ± 19.2 (2.1-67.4)	106.9 ± 71.6 (2.0-349.3)	91.8 ± 62.7 (0.2-291.4)	100.4 ± 67.8 (2.2-343.5)	110.8 ± 66.5 (3.6-335.9)

[1], Units: $\mu g\ m^{-3}$ except CO units: $mg\ m^{-3}$

[2], $PM_{2.5}$ and PM_{10} from IAP and Pinggu measured by a gravimetric method; all other data are online measurements hourly mean.

Table 5: Mean and standard deviation (sd) of climatological conditions in Beijing for each circulation type (CT) for 1988-20 17 from Era Interim data with frequency of the CT during the W (winter) and S (summer) campaigns (% of 6 h periods (p)) compared to A- long- term 1988-2017.

CT	Description	WS m s^{-1}	WS_{sd} m s^{-1}	WD °	WD_{sd} °	T2m °C	$T2m_{sd}$ °C	TD2m °C	$TD2m_{sd}$ °C	MSLP hPa	$MSLP_{sd}$ hPa	RH %	RH_{sd} %	Season	Frequency (%) W	S	A
1	H - west of the domain	3.38	1.63	298.3	62.6	0.1	7.1	-12.6	7.9	1026.50	4.14	41	18	Winter monsoon	16	7	9.3
2	H - west of the domain	2.91	1.49	265.9	107.0	-2.8	6.2	-13.8	7.5	1034.34	4.47	45	18	Winter monsoon	1	0	7.2
3	relatively L in NE	3.21	1.65	281.2	71.3	6.8	8.9	-6.4	9.3	1017.77	4.35	43	20	Sep- May	12.5	0	8.3
4	further reduction L (cf. CT3, 5) in NE winds start to turn over Yellow Sea	3.05	1.73	240.1	104.1	19.2	7.5	7.0	10.4	1007.20	3.63	50	24	Mar-Aug Spring - summer	11.8	4	7.8
5	relatively L in NE	2.57	1.37	189.1	125.0	8.2	8.9	-0.9	10.4	1020.82	4.62	57	23	Sep-May	7.6	34	8.3
6	further reduction L (cf. CT3, 5) in NE	2.58	1.32	197.4	87.6	24.6	5.9	14.7	8.0	1000.99	2.96	59	23	Summer monsoon	8.3	12	8.9
7	when winds are oriented westward from the Bohai Sea	2.29	1.12	167.5	100.2	18.9	7.8	10.7	9.5	1012.59	3.61	63	21		1 p	11	10.2
8	like CT 6	2.35	1.11	165.4	75.4	24.0	5.3	15.9	6.8	1006.47	2.69	65	21	Summer monsoon		32	12.9
9	Air mass stagnant over Beijing	2.03	0.94	208.7	107.4	2.1	7.9	-6.2	8.4	1028.66	4.18	58	20			0	9.6
10	Air mass stagnant over Beijing	2.67	1.17	211.1	68.7	14.2	9.4	3.1	10.0	1013.98	3.84	52	22		25	0	7.2
11	Air mass stagnant over Beijing	2.23	0.98	209.1	86.5	8.1	9.4	-0.4	9.6	1021.83	4.06	59	20		16	0	10.3

Note: WS- wind speed, WD wind direction, T2m – 2 m air temperature, TD2m – 2 m dewpoint temperature, MSLP – mean sea level pressure, RH – relative humidity; L – low pressure; H – High pressure

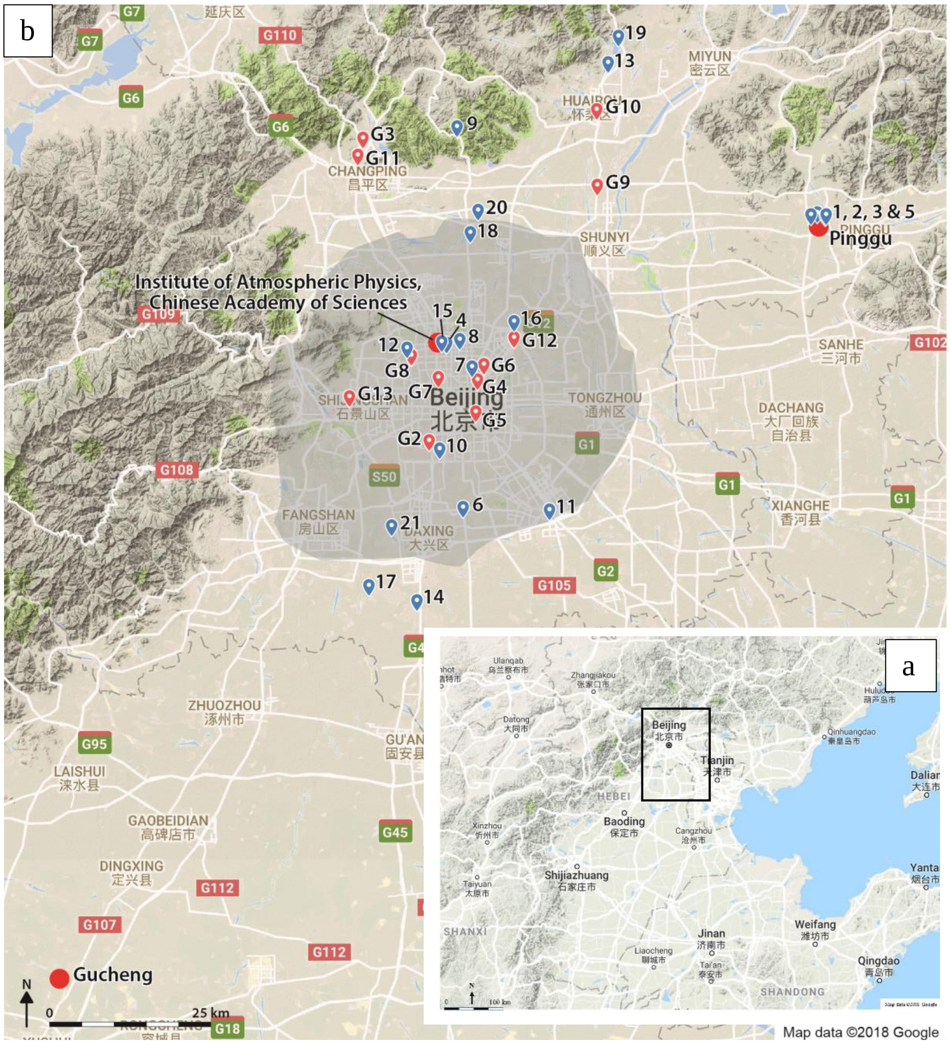
b
a
Institute of Atmospheric Physics,
Chinese Academy of Sciences
Beijing
北京
Pinggu
Gucheng
1, 2, 3 & 5
4
6
7
8
9
10
11
12
13
14
15
16
17
18
19
20
21
G2
G3
G4
G5
G6
G7
G8
G9
G10
G11
G12
G13
MIYUN
密云区
CHANGPING
昌平区
SHUNYI
顺义区
SANHE
三河市
TONGZHOU
通州区
DACHANG
大厂回族
自治县
XIANGHE
香河县
FANGSHAN
房山区
DAXING
大兴区
ZHUOZHOU
涿州市
GU'AN
固安县
LAISHUI
涞水县
GAOBEIDIAN
高碑店市
DINGXING
定兴县
N
0
25 km
Beijing
北京市
Tianjin
天津市
HEBEI
Baoding
保定市
Shijiazhuang
石家庄市
SHANXI
Jinan
济南市
Weifang
潍坊市
Qingdao
青岛市
SHANDONG
Map data ©2018 Google

Atmos. Chem. Phys. Discuss., https://doi.org/10.5194/acp-2018-922
Manuscript under review for journal Atmos. Chem. Phys.
Discussion started: 15 October 2018

Atmospheric Chemistry and Physics
Open Access
Discussions

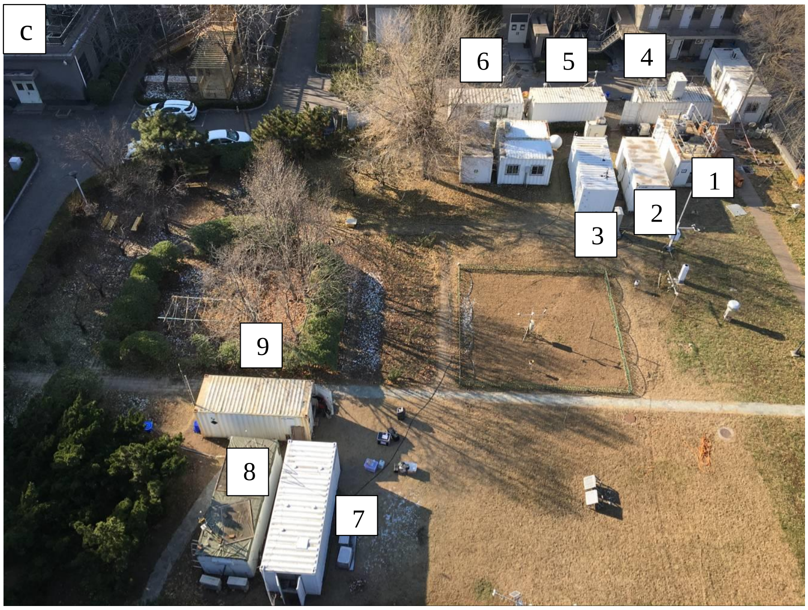

Figure 1: Study area topography (source: googlemap) of Beijing / Tianjing / Hebei region (a) with the rectangle showing enlarged study area; locations of measurement sites (Institute of Atmospheric Physics (IAP)– urban Beijing, Pinggu – rural Beijing; and Gucheng – upwind site in Hebei province), SNAQ box sites (red symbols) and the 12 national air quality monitoring stations (G1 to G12, blue symbols) (b); locations of the 9 containers at IAP (c) – instrumentation at each container is shown in Table 1. The shaded area shows the Beijing buildup area. (Source: a and b - Goggle Map topographic background imagery; c – taken by ~~Siyao Yue~~ Jian Zhao from IAP).

G1: Wangshouxigong; G2: Dingling; G3: Dongsi; G4: Tiantan; G5: Nongzhanguan; G6: Guanyuan; G7: Haidianquwanliu; G8: Shunyxicheng; G9: Huairouzhen; G10:Changpingzhen; G11: Aotizhongxin (Olympic Park); G12: Gucheng. Categories: Urban: G1, G3, G4, G5, G6, G7, G8, G11, G12; Suburban: G9, G10; Rural: G2.

Atmos. Chem. Phys. Discuss., https://doi.org/10.5194/acp-2018-922
Manuscript under review for journal Atmos. Chem. Phys.
Discussion started: 15 October 2018

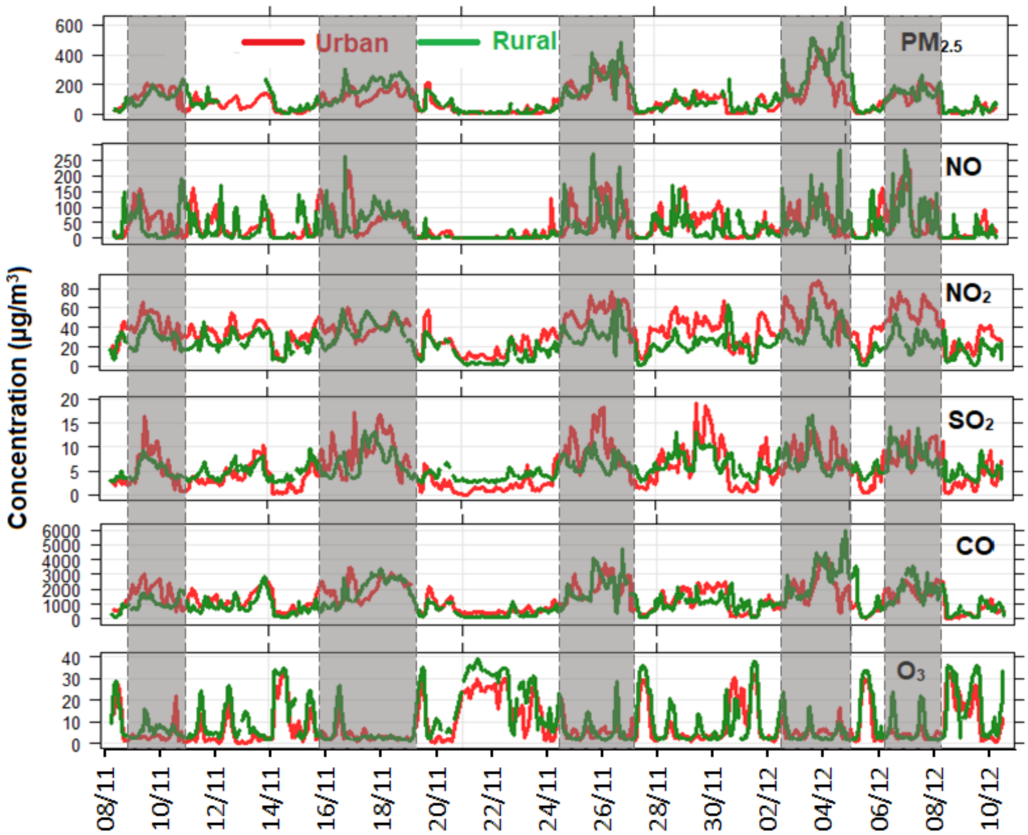

Figure 2: Time-series of air quality variables at the urban and rural sites during the winter campaign; Five haze events are indicated (shading).

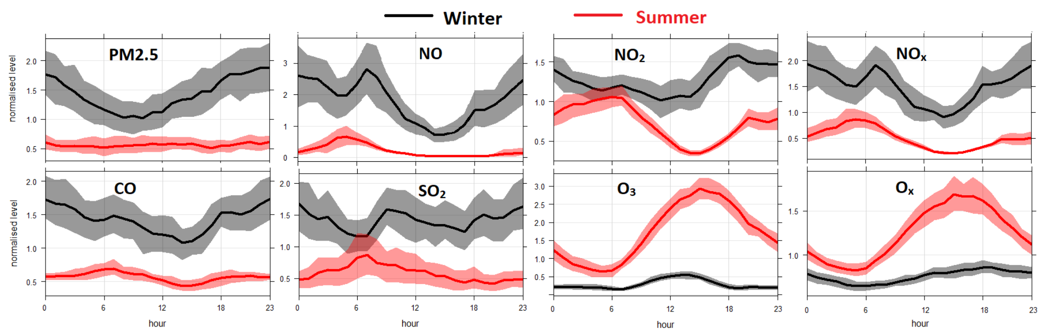

Figure 3: Diurnal patterns of gaseous pollutants normalized by average concentrations at IAP during winter and summer campaigns. Line shows the mean concentrations and shaded area as 95% confidence interval in the difference in mean concentrations.

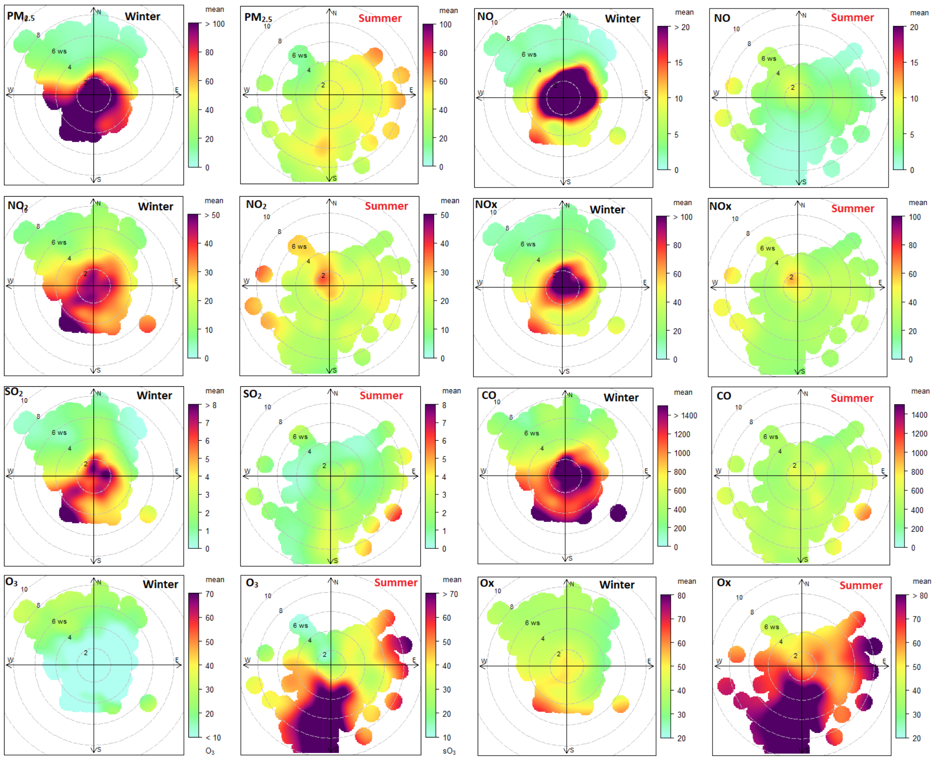

Figure 4: Air pollutants concentration (colour) with wind direction (angle) and wind speed (m s^{-1}) at IAP during the winter and summer campaigns. Data are hourly in time resolution and were from 10 November to 11 December 2016 (winter) and 21 May to 22 June 2017 (summer). The colour scale is for "weighted.mean" where the mean wind speed/direction bin is multiplied by the bin frequency and divided by total frequency.

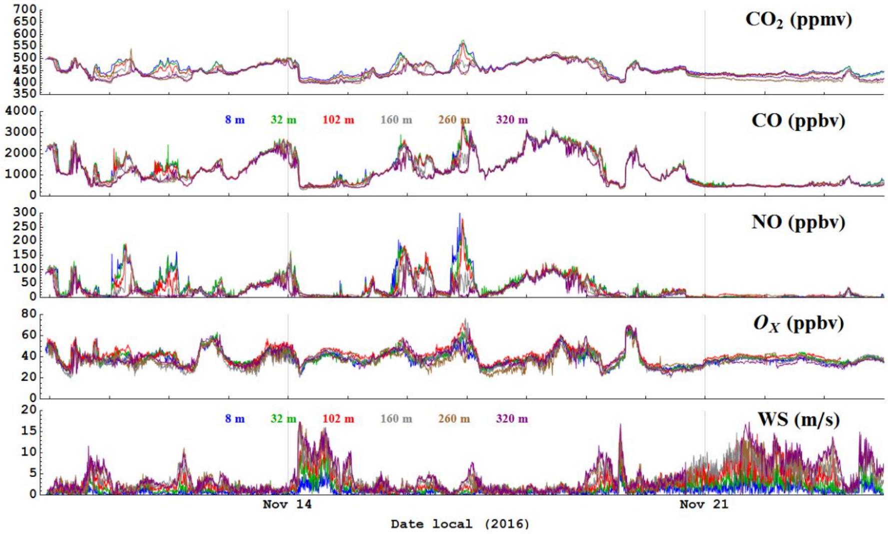

Figure 5: Time series of CO_2, CO, NO, O_x (NO_2+O_3) and wind speed at six heights (colour) measured with SNAQ boxes on the IAP tower during the winter intensive field campaign.

Atmos. Chem. Phys. Discuss., https://doi.org/10.5194/acp-2018-922
Manuscript under review for journal Atmos. Chem. Phys.
Discussion started: 15 October 2018

Atmospheric Chemistry and Physics
Discussions
Open Access

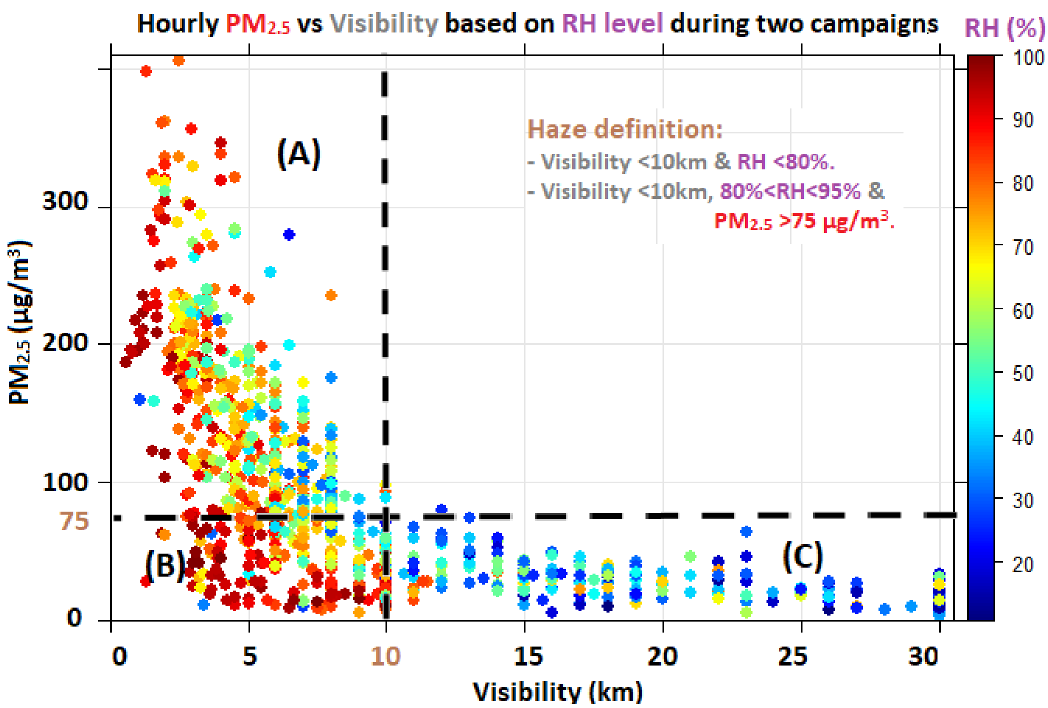

Figure 6: Hourly $PM_{2.5}$ mass concentrations versus visibility (at the Beijing Capital Airport) during the winter campaign. Data source: visibility downloaded using R-"worldmet" package: date of last access: 27/02/2018).

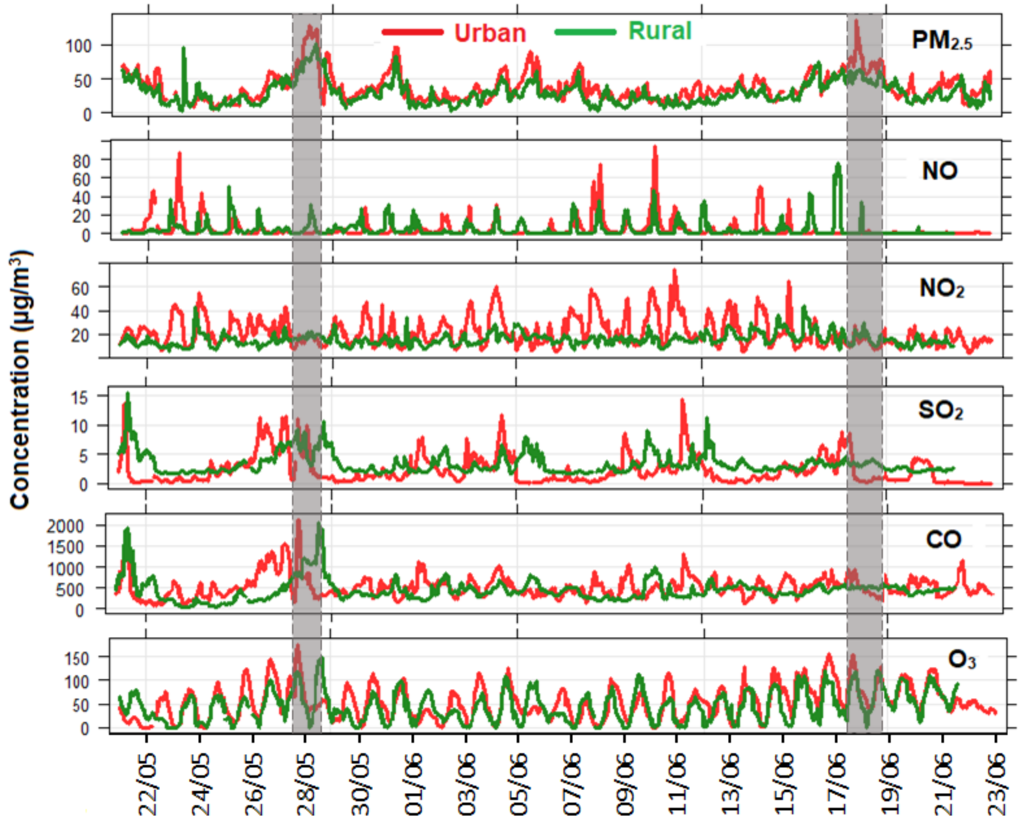

Figure 7: Time-series of air quality variables at the urban and rural sites during the summer campaign. Two minor haze events are indicated (shading).

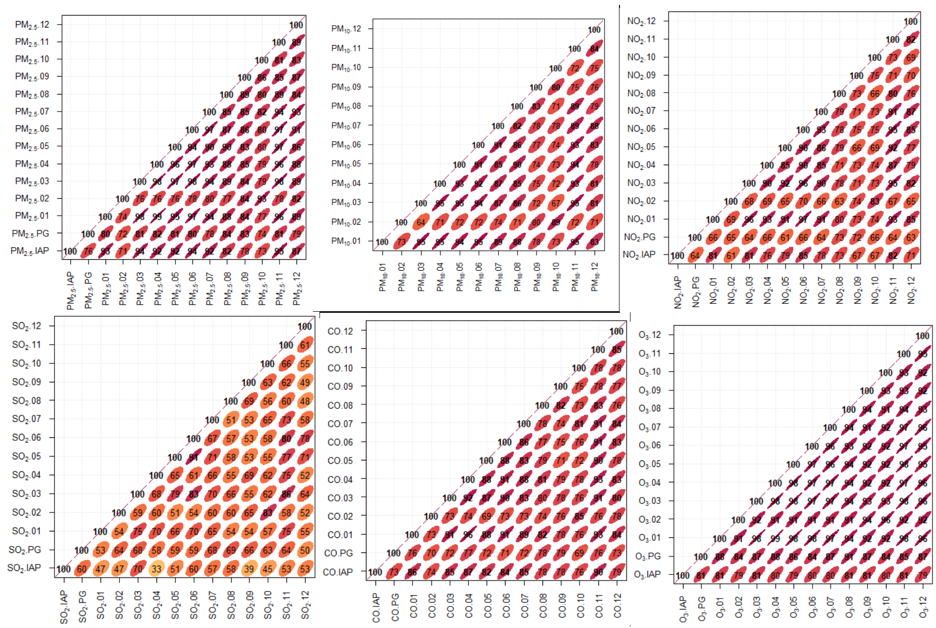

Figure 8: Correlations between the air quality at IAP, PQ and 12 monitoring station around Beijing. Stations G1-G12 (Figure 2) are labelled 01-12, PG = Pinggu.

Atmos. Chem. Phys. Discuss., https://doi.org/10.5194/acp-2018-922
Manuscript under review for journal Atmos. Chem. Phys.
Discussion started: 15 October 2018

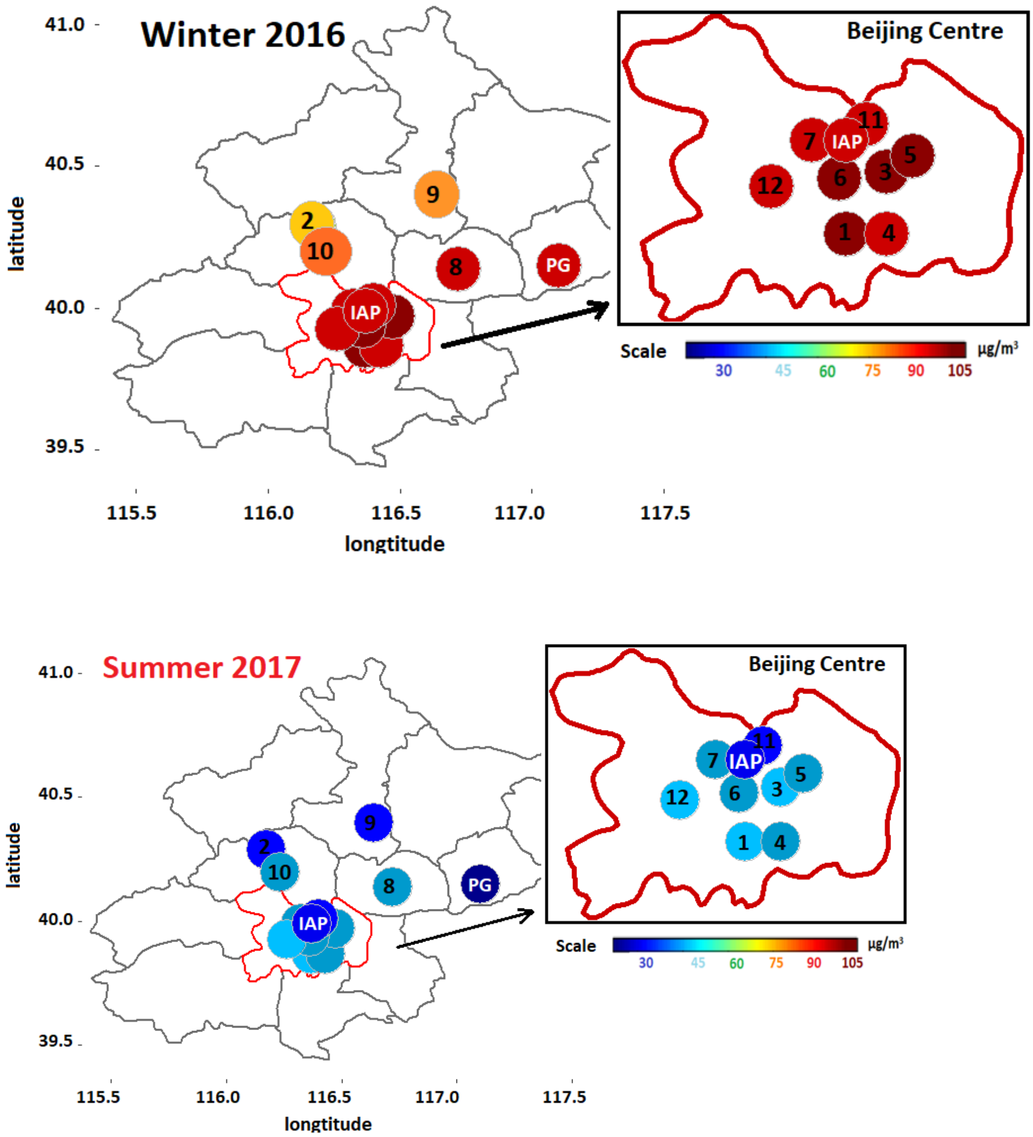

Figure 9: Spatial distribution of hourly mean concentration of $PM_{2.5}$ in Beijing during two sampling campaigns.

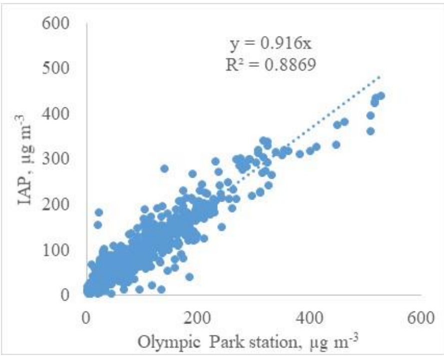

Figure 10: Hourly $PM_{2.5}$ at IAP (roof of a two storied building) and the neighbouring Olympic park national air quality monitoring station during the winter and summer intensive field campaigns.

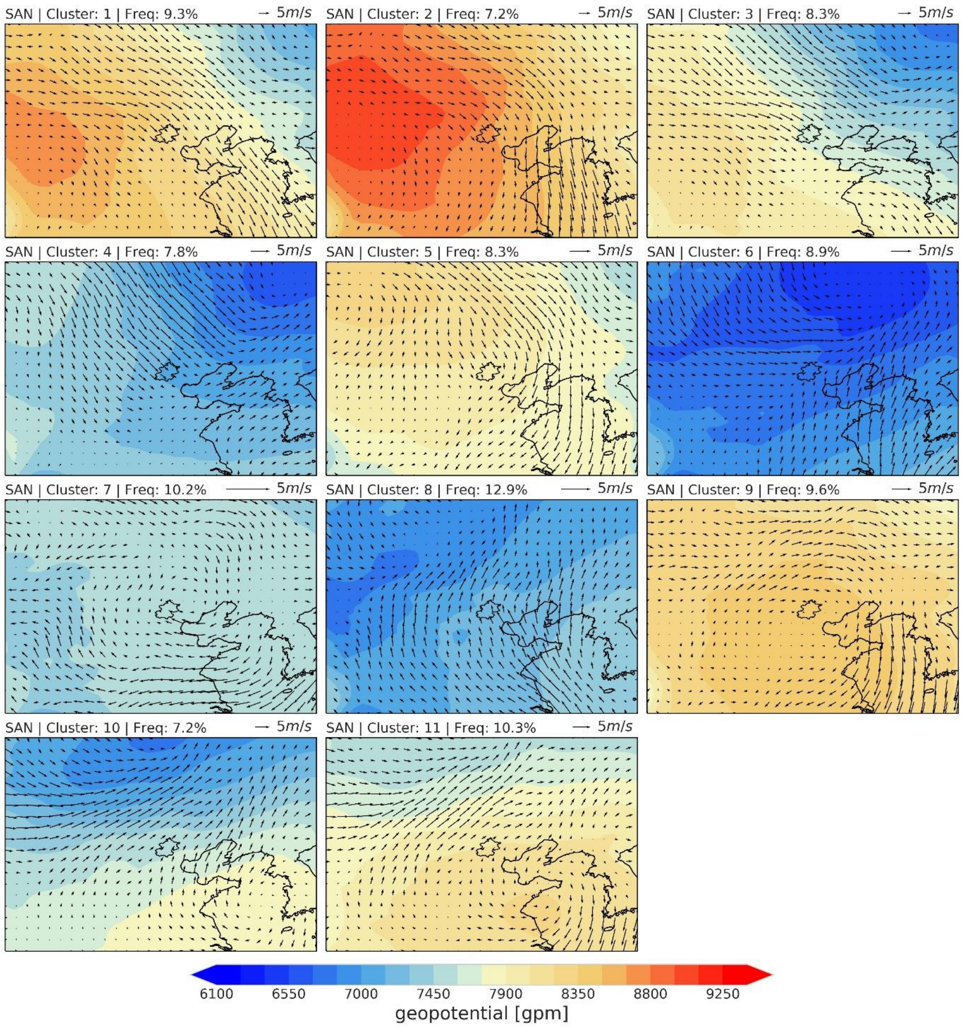

1329

1330 **Figure 11:** ERA-Interim (1988-2017) average 925 hPa geopotential with 10 m horizontal wind
1331 vector for 11 circulation types classified for Beijing (municipal boundary thin solid line)
1332 surroundings (103-129° E, 31 - 49° N) determined with the SANDRA method (COST733 class
1333 software). Frequency of occurrence is given in cluster caption. For discussion of conditions
1334 associated with each CT see section 6.1.
1335

Atmos. Chem. Phys. Discuss., https://doi.org/10.5194/acp-2018-922
Manuscript under review for journal Atmos. Chem. Phys.
Discussion started: 15 October 2018

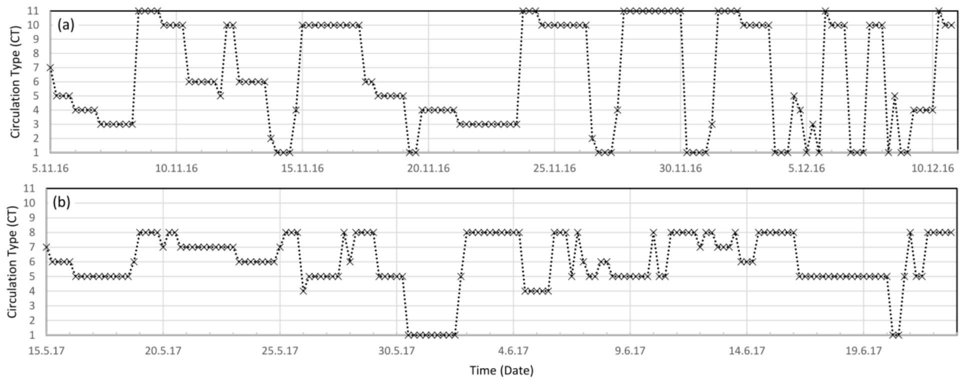

Figure 12: Time series of circulation types (CTs) during the two field campaigns: (a) winter and (b) summer. The 11 CTs are shown in Figure 11. See text for more description.

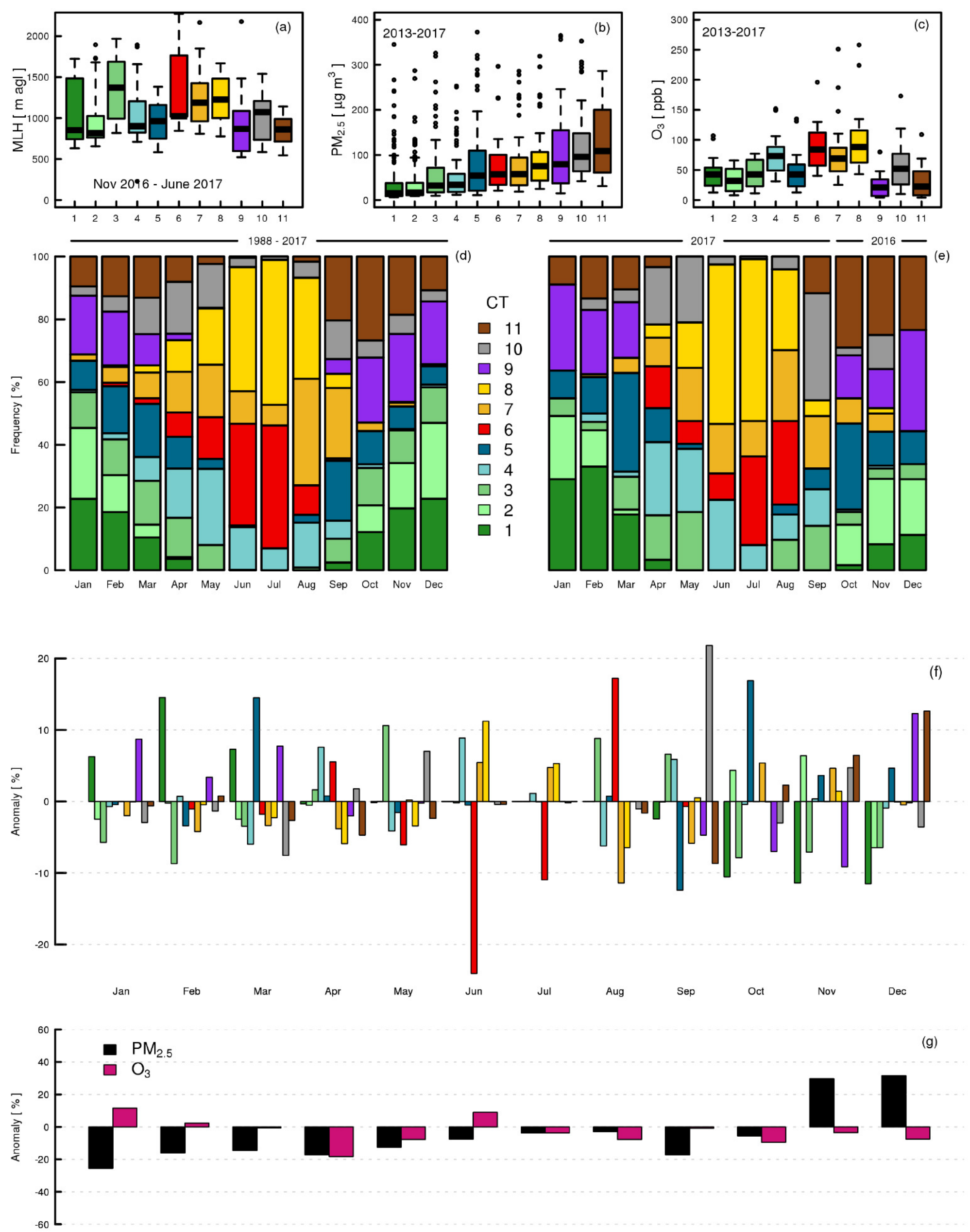

Figure 13: Analysis by circulation type (CT; Sect. 0) of: (a) daily maximum mixed layer height (MLH) determined from ALC observations at IAP between November 2016 – June 2017 (analysis method, Kotthaus and Grimmond, 2018b); concentration of (b) $PM_{2.5}$ and (c) O_3 at at the Olympic Park (i.e. Aotizhongxin) in 2013-2017 from the national air quality network; occurrence of CTs in (d) 1988-2017 and (e) Oct 2016 – Sept 2017; (f) anomaly of CT frequency during Oct 2016 – Sept 2017 compared to 30 y climatology; and (g) anomaly of $PM_{2.5}$ and O_3 during Oct 2016 – Sept 2017 compared to 5 y (2013-2017) average (same data as in b, c).

Atmos. Chem. Phys. Discuss., https://doi.org/10.5194/acp-2018-922
Manuscript under review for journal Atmos. Chem. Phys.
Discussion started: 15 October 2018

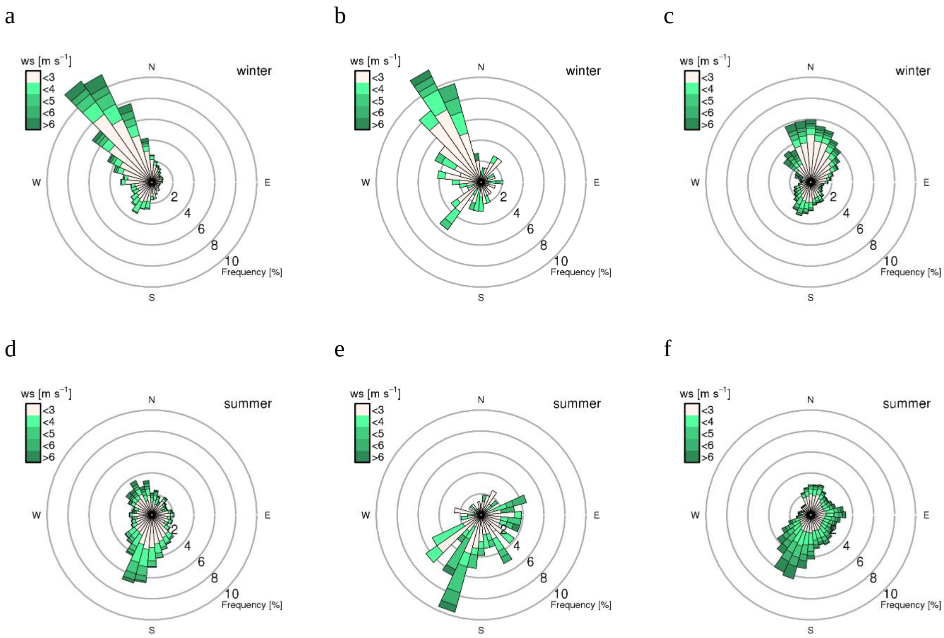

1351

1352 **Figure 14:** Beijing wind roses: (a, b, d, e) ERA-Interim 10 m horizontal wind (40° N, 116.5° E)
1353 and (c, f) sonic anemometer (Table 1) at IAP 320 m agl for (a) 5 November – 10 December in
1354 1988-2017, (d) 15 May – 22 June in 1988-2017, (b, c) 5 November – 10 December 2016, and (e, f)
1355 15 May – 22 June 2017.

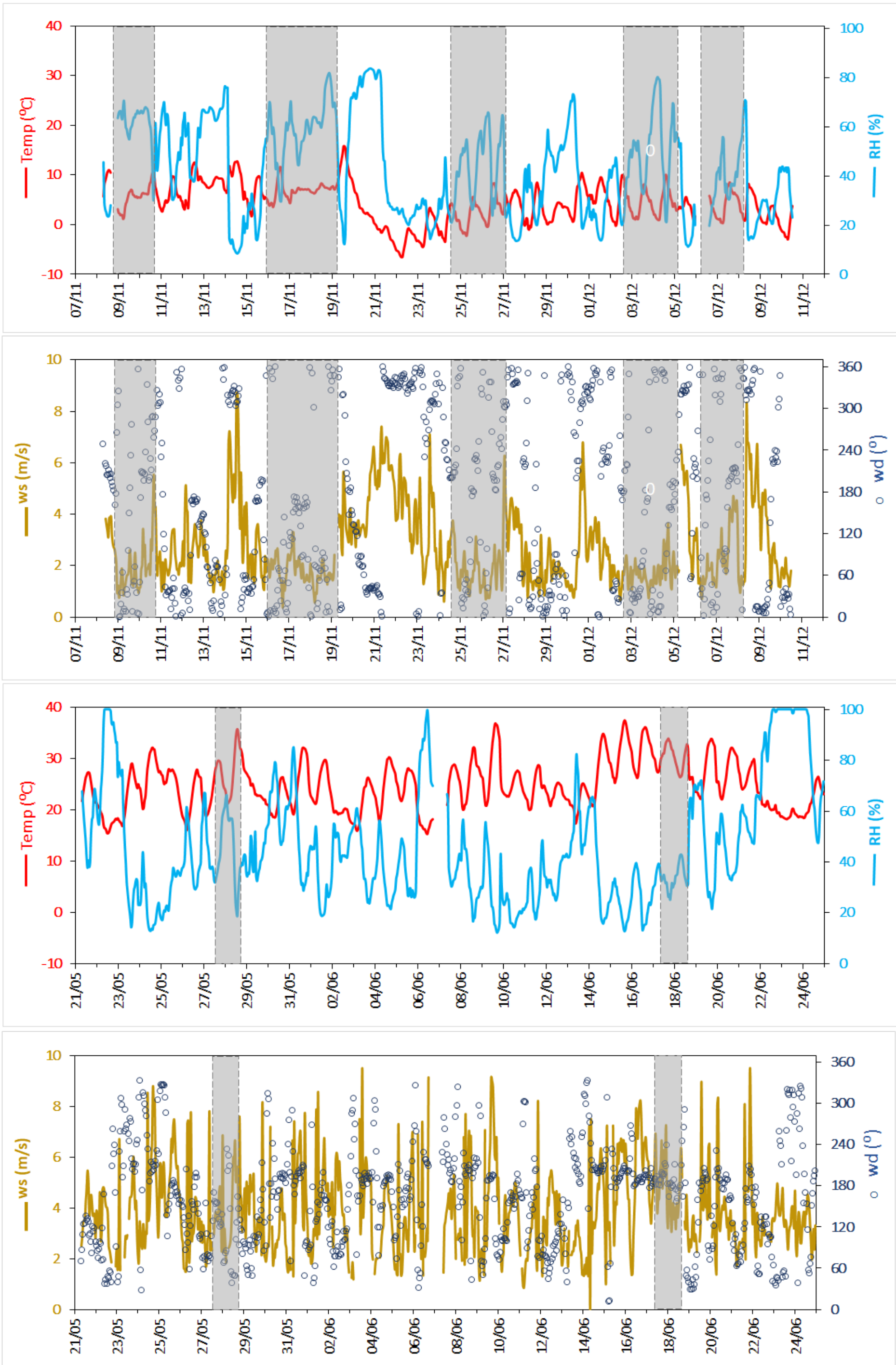

Figure 15: Hourly meteorological variables measured at 120 m during the (a) winter and (b) summer campaigns. The shaded areas highlighted the haze periods (Table 3, Figures 2 and 7).

Atmospheric Chemistry and Physics
Discussions
Open Access

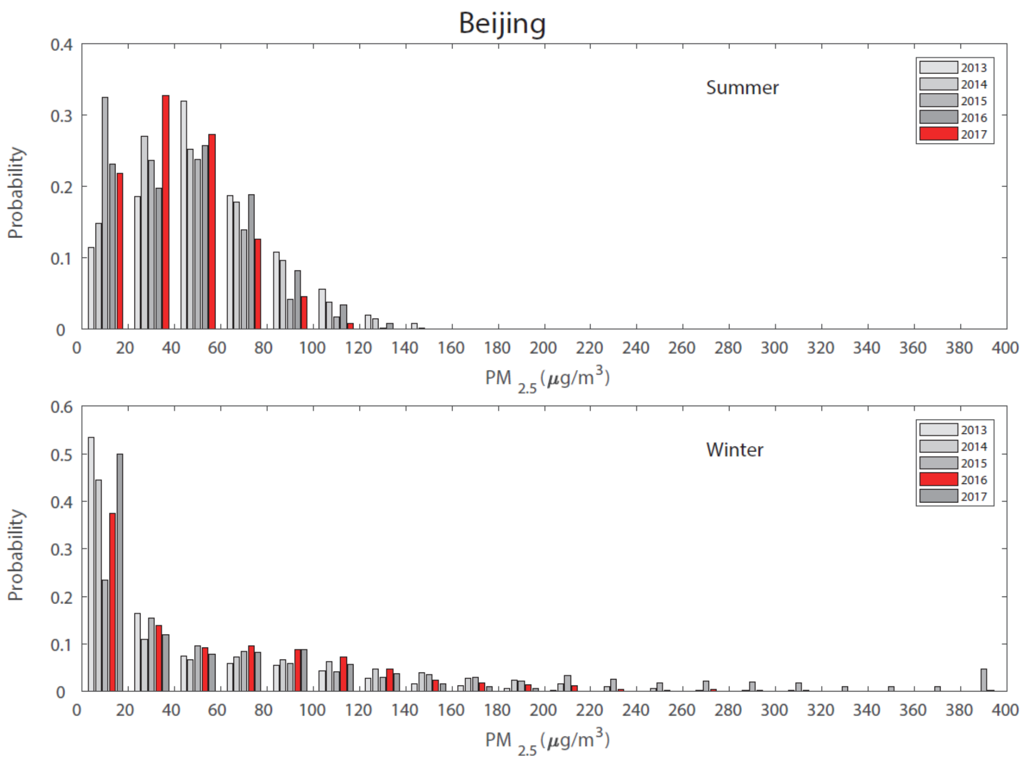

Figure 16: Frequency distribution of $PM_{2.5}$ in Beijing over the summer (top) and winter (bottom) campaign periods from the NAQPMS model compared with those from the same periods over the past five years under the same emission conditions